



Revisiting the dry-to-wet shift of summer precipitation over the Three-River Headwaters region, hinterland of the Tibetan Plateau: a perspective of moisture sources changes

Ruiyu Zhao^{1,2} · Bin Chen¹ · Wei Zhang³ · Hongli Ren¹ · Yang Zhao⁴ · XiangDe Xu¹

Received: 14 February 2024 / Accepted: 21 July 2024

© The Author(s), under exclusive licence to Springer-Verlag GmbH Germany, part of Springer Nature 2024

Abstract

The Three-Rivers Headwater (TRH) region has experienced notable dry-to-wet shift in summer precipitation in recent decades. Despite the widespread efforts of scientific community, the causes of such climate shift remain not well-understood. Building upon an ensemble of high-resolution Lagrangian simulations and moisture source diagnostic, this study investigated the long-term changes in moisture sources with the ERA-Interim reanalysis from 1980 to 2017, particularly aiming to pose a complimentary understanding on this shift from a perspective of moisture source changes. The results show that the variability of moisture sources for the water vapor reaching the TRH region is closely and quantitatively linked to its regional summer precipitation. The dry-to-wet shift in summer precipitation in TRH is regulated by the changes in moisture sources across multiple transport time scales (from 1 to 10 days), and could be attributed to the enhanced contribution by the moisture sources originated from the Tibetan Plateau (TP), the Central Eastern Asian region (CEA), and the Arabian Peninsula (ARP), of which regional accumulative moisture contribution increased by 11.3 (0.33%), 8.61 (0.27%) and 8.53 (0.52%) mm per year, respectively. This result implies that the terrestrial source ranks the leading role in regulating the decadal shift of TRH summer precipitation, rather than that directly from the oceanic regions. Although the moisture sources are across multiple transport timescales, the relatively shorter transport distance and steady contribution (lasting 1 to 10 days) from the TP highlight the significance of strengthened local precipitation recycling process in this dry-to-wet shift. Further analysis indicates the variations in mid-latitude meridional winds and the low-latitude SST play a role of ‘bridge’ connecting the changes in moisture sources to enhanced precipitation during the summer season.

Key points

- 1) The decadal variation of regional precipitation over the TRH region is closely and quantitatively linked with the changes in moisture sources.
- 2) The moisture sources responsible for the dry-to-wet shift in summer rainfall over the TRH have been detected.
- 3) The weakened mid-latitude meridional winds and the warming low-latitude sea surface temperature bridge the moisture source changes and summer precipitation over the TRH region.

✉ Bin Chen
chenbin@cma.gov.cn

¹ State Key Laboratory of Severe Weather, Chinese Academy of Meteorological Sciences, Beijing, China

² Department of Atmospheric and Oceanic Sciences, Institute of Atmospheric Sciences, Fudan University, Shanghai, China

³ Utah State University, Logan, Utah, USA

⁴ Frontier Science Center for Deep Ocean Multispheres and Earth System and Physical Oceanography Laboratory and College of Oceanic and Atmospheric Sciences, Ocean University of China, Qingdao, China

1 Introduction

The Tibetan Plateau (TP), with an average altitude of more than 4000 m above sea level, is well known as the “Roof of the World” or “The Third Pole” (Xu et al., 2008, 2014; Yao et al., 2019). The Three-Rivers Headwater (TRH) region, located in the hinterland of the TP (Fig. 1), is also known as the “Asian Water Tower” since it is the original region of the Asia’s major rivers, such as the Yangtze River, the Yellow River, and the Lancang-Mekong River (Xu et al., 2008;

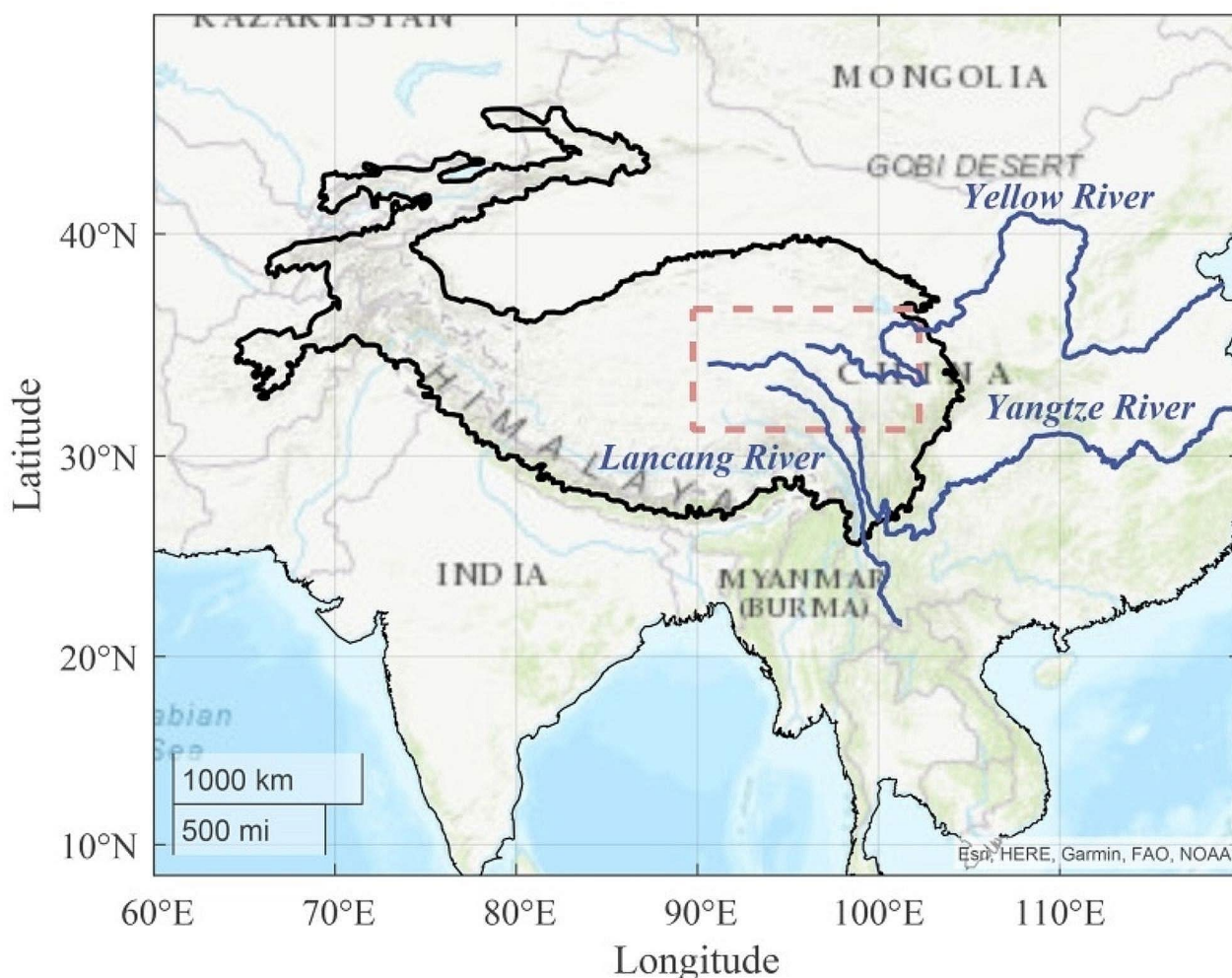


Fig. 1 Geographical location of TRH region (red dashed rectangle), together with the Yellow River, Yangtze River, and Lancang River (blue lines). The black thick contour indicates the topographic height of 2000 m, which roughly represents the TP

Immerzeel et al. 2010; Yao et al., 2012; Curio and Scherer 2016). TRH region is an important reservoir of freshwater resources in China, delivering about 42.5 billion tons of freshwater downstream every year (Wang et al., 2007; Chen et al. 2015).

Under a changing climate, the temperature of the “Asian Water Tower” experiences a warming rising at a rate of 0.42 °C per decade, approximately twice the global average warming rate (Yao et al. 2022), resulting in the retreated glaciers and degraded permafrost (Immerzeel et al., 2010, 2020; Yang., 2014). With this amplified warming, the precipitation frequency and intensity in the TRH region demonstrate a significant variability and uncertainty (Yi et al. 2013; Zhao et al. 2021; Kukulies et al. 2023; Liu et al. 2023), thereby exerting profound impacts on regional hydrological and ecological cycles (Xu et al. 2019; Shao et al. 2017), and thereby altering the fresh water supply for billions of people dwelling in downstream areas (Qiu 2008). Therefore,

understanding the characteristics of precipitation variability and associated underlying mechanisms in the context of global warming is of great scientific value and practical significance for improving water resources management and ecosystem stability over the TRH region.

Precipitation variability in the TRH region has been one of the research hotspots for academic community in the atmospheric fields (Yang et al. 2014; Ma et al. 2018; Xi et al. 2018; Li et al. 2020). A large number of previous studies have explored the characteristics of precipitation variations across multi-spatiotemporal scales (e.g., Yi et al. 2013; Shi et al. 2017; Xi et al. 2018; Li et al. 2020; Lai et al. 2021; Meng et al., 2022; Yu et al. 2023; Xu et al. 2024). The results demonstrated that the precipitation in the TRH region has clearly shown an increasing trend (Dong et al. 2020; Liu et al. 2019; Tong et al. 2014; Sun et al., 2018; Zhao et al. 2023), potentially leading to the expanded lakes in the inner TP (Lei et al. 2013, 2014; Yang et al. 2018; Qiao

et al. 2019). Particularly for the summer season, the precipitation over this region is featured by a decadal dry-to-wet transition (Zhao et al. 2023; Liu et al. 2023) due to the enhanced frequency of extreme precipitation events (Zhao et al. 2021; Liu et al. 2023).

Strenuous efforts have been devoted to revealing the causes of the long-term variation in precipitation over the TRH region and its underlying mechanisms from the angle of anomalous atmospheric conditions (e.g., Liu et al. 2015; Sun et al., 2018; Zhou et al. 2019; Dong et al. 2020; Sun et al. 2020; Yue et al. 2021; Shang et al., 2022; Liu et al., 2022; Li et al. 2024). More specifically, the anomalous wave trains accompanied by simultaneously weakened East Asian westerlies over the TP (Zhou et al. 2019; Sun et al. 2020; Liu et al., 2022), together with the changes in sea surface temperature (SST) over the Indo-Pacific warm pool (Yue et al. 2021) and Atlantic (Shang et al., 2022; Wang et al., 2022) have been considered as essential factors in modulating decadal variability of TRH regional precipitation. The TRH region is an intricate area influenced by the mid-latitude westerlies and the Asia summer monsoon systems. Although those previous studies have documented decadal precipitation variations, the reasons behind decadal dry-to-wet changes in summer precipitation in the TRH region are still largely unclear and warrant further study (Yang et al. 2014; Ma et al. 2018; Wang et al. 2018).

In addition to the impacts of anomalous atmospheric conditions, the global warming has affected the hydrological water cycle and then profoundly altered the amount of precipitation over most regions in the world (Held and Soden 2006). Given that a large supply of water vapor is considered a prerequisite for precipitation formation (Gimeno et al. 2012), it can be speculated that this dry-to-wet transition in precipitation in the TRH region could be directly attributed to more water vapor supply, departing from either the internal or external moisture origins (Gao et al. 2014). Taking the TP region as a whole, studies have explored the processes of the atmospheric water cycle and its connection to precipitation changes using the Eulerian approach (Feng and Zhou., 2012; Curio et al. 2015; Pan et al. 2019; Zhang et al. 2019a; Li et al. 2022) or the Lagrangian method (e.g., Chen et al. 2012, 2019; Gao et al. 2014; Zhang et al. 2017, 2019; Liu et al. 2020; Yang et al. 2020; Liu et al., 2022). A recent research by Wang et al. (2023) stated that the enhanced atmospheric water cycle processes are caused by climate warming in the TRH region. However, the atmospheric water cycle and its relationship with the precipitation in the TRH region were comparably less explored. Some studies have shown that, in addition to the middle latitude westerly and the northwestern airflow transporting from Eurasia, the moisture reaching the TRH region is mainly conveyed by the southwestern water vapor transport from the Indian Ocean, the Arabian Sea and

the Bay of Bengal (Li et al. 2009; Quan et al. 2016; Zhang et al. 2019b). The changes in water vapor transport are well in coincidence with the precipitation variation in the TRH region on the annual scale (Chen et al. 2022; Zhao et al. 2023). More recently, Zhang et al. (2019c) found that the southwestward water vapor transport from the Indian Ocean contributes about 51.4% of the precipitation in the southern TP. The increased southwesterly water vapor transport through the southern boundary of the TRH region is one of the factors responsible for the dry-to-wet transition of summer precipitation over this region (Liu et al. 2023; Wang et al. 2023). Previous research mentioned above provides us valuable insights on the variation in summer precipitation; however, to the best of our knowledge, the relative contributions of moisture sources changes to precipitation in the TRH region remain uncertain.

Considering that the moisture sources serve as the main component of water cycle and an essential prerequisite of precipitation, the knowledge on the origin of water vapor leading to the rainfall over a target region could promote a better understanding of the precipitation variations (Gimeno et al. 2020). Thus, the moisture origins identification in the TRH and quantification of their contributions to the decadal precipitation transition over the THR merit further exploration. For a better understanding of the causes of the decadal dry-to-wet transition in summer precipitation over the TRH, this study is thereby trying to address the following two questions:

- 1) What are the main enhanced moisture sources that are responsible for the dry-to-wet transition of summer precipitation in the THR region?
- 2) What is the linkage between decadal changes in moisture sources and the atmospheric condition over the THR region?

The rest of this paper is arranged as follows. Section 2 describes the data, model and methods utilized in this study. Section 3 examines dry-to-wet transition of summer precipitation in the TRH region and its association with the moisture sources, together with the circulation factors regulating the decadal dry-to-wet transition of summer precipitation. Section 4 discusses the results of this study and some caveats. The summary and conclusions are presented in Sect. 5.

2 Data, model and method

2.1 Datasets

To quantify the characteristics of dry-to-wet transition in summer precipitation, this study adopts a quality-controlled

monthly precipitation data set with a spatial resolution residing on $0.5^\circ \times 0.5^\circ$ latitude-longitude grids. This dataset is released and routinely updated by the National Meteorological Information Center (NMIC) of the China Meteorological Administration (NMIC/CMA, <http://data.cma.cn/>). Overall, this dataset has proven to be of good quality, because the generation process is subjected to rigorous quality control.

The ERA-Interim reanalysis derived from the European Centre for Medium-Range Weather Forecasts (ECMWF) project (Dee et al. 2011) is used as the meteorological fields to drive the Lagrangian transport mode FLEXPART. These fields are embedded on 60 hybrid model levels ranging vertically from the surface to 0.1 hPa with a longitude/latitude grid resolution of $0.75^\circ \times 0.75^\circ$ at 6-hour interval. The ERA-Interim reanalysis performs well in describing the processes of atmospheric water cycle in the TP (Gao et al. 2014). Moreover, the monthly fifth-generation ECMWF dataset with a spatial resolution of $0.25^\circ \times 0.25^\circ$ is utilized to diagnose the atmospheric physical variables, including the vertically integrated moisture transport, sea surface temperature (SST), geopotential height, vertical velocity, and wind vectors. All the data are collected with a span of 1980–2017.

2.2 Lagrangian trajectory model and its configuration

The Lagrangian transport and dispersion model (FLEXPART) is adopted to carry a 38-year modeling. FLEXPART model is suitable for the simulation of a large range of atmospheric transport processes (<https://www.flexpart.eu/>). It differs from the typical model of calculating the trajectory of a single point, but by calculating the trajectory of a group of air parcels, thereby realizing the simulation of the transport and diffusion process of atmospheric substances covering a three-dimensional region (Stohl and Seibert., 1998). Currently, FLEXPART has been widely applied in the research fields of the atmospheric water cycle, in particular for moisture sources identification (e.g., Stohl and James, 2004, 2005; Chen et al. 2012; Gimeno-Sotelo et al., 2022; Liu et al., 2022).

In this study, the Lagrangian model is initialized with a domain-filling technique, namely the three-dimensional space of the region (-20 – 60°N and 0 – 160°E) is divided into roughly 2.0 million air parcels with equal air mass. Under the forcing of three-dimensional wind fields, all the air parcels are moved freely. For each summer season, the Lagrangian modeling starts starting on May 1 and ends on September 31. Since the water vapor residing in the circulation cycle is on an average of 10-day (Trenberth., 1999), all the air parcels reaching the TRH region during the summer season (June–August) are traced backward for 10 days. The

modeling outputs for each air parcel are stored in 3-hour intervals, including the three-dimensional position (latitude, longitude, and altitude), as well as the information on physical quantities such as temperature, specific humidity, and air mass.

2.3 Methods

a. Moisture Source Diagnosis

The diagnostic of the moisture sources is based on the changes in the specific humidity along the trajectories. By considering the temporal sequence of evaporation and precipitation in an air parcel during transport, Sodemann et al. (2008) proposed a new Lagrangian methodology for the identification of the moisture sources for precipitation, which allows for a quantitative demarcation of evaporative moisture sources. In this study, building on the FLEXPART model output, all the particles entering or residing over the TRH (31.25°N – 37.25°N , 89.25°E – 102.75°E) during the boreal summertime from 1 June to 31 August of 1980–2017 are selected and considered for further analysis. For each air parcel selected, the increases (e) and decreases (p) in moisture along the backward trajectory may be calculated from the changes in (q) with time ($e - p = m(dq/dt)$), where m is the mass of the parcel. The locations of positive changes along the trajectory path are considered as the points of moisture uptake. By summing all the values of ($e - p$) for the parcels selected in a given atmospheric column over an area, it is possible to obtain ($E - P$),

$$E - P = \frac{\sum_{i=1}^N m \frac{\Delta q}{\Delta t}}{A}$$

To quantify the impact of these processes on the analyzed source regions, a calculation of the fractional contribution of each source is performed, following the method of Sodemann et al. (2008), taking the possibility of multiple recycles into account. Thus, a 6-h database of trajectories entering into TRH region is constructed with the 38-summer $E - P$ values in the $1^\circ \times 1^\circ$ latitude-longitude grids, and then averaged to summer seasonal composite maps. The back trajectory $E - P$ values of the previous day number n are denoted with $(E - P)_n$. For example, $(E - P)_1$ represents the total gain or loss of moisture on the previous day along the back trajectories. Accordingly, $(E - P)_{1-n}$ indicates the integrated value of $(E - P)$ from 1 to n days in backward tracking time.

b. Atmospheric circulations Index

To characterize the variation of atmospheric circulations, the Silk Road Index (SRI) is defined as the normalized principal component of the first empirical orthogonal function mode (EOF1) of the summer mean meridional wind on 200 hPa level over the limited region (20°–60°N, 30°–130°E; Kosaka et al. 2009).

Additionally, the Indo-Pacific Warm Pool (WPI) Index is derived from NOAA (<https://psl.noaa.gov/data/climateindices/list/>), which is considered as the areal mean of Sea Surface Temperature (SST) over the domain of 60°E–170°E, 15°S–15°N (Martin et al. 2010). The Pacific Decadal Oscillation (PDO) index is defined by the leading pattern (EOF) of SST anomalies in the North Pacific basin (typically, polewards of 20°N). The SST anomalies are obtained by removing both the climatological annual cycle and the global-mean.

c. Analyzing methods

The time series of precipitation is commonly non-stationary signals containing multiple time scales (Huang et al. 1998). To decompose the decadal signal from their periodic oscillations, we adopt the EEMD analysis method to perform a time-frequency analysis (Wu and Huang 2009; Qian and Zhou 2014). Here, the precipitation series is decomposed into four IMF (Intrinsic Mode Function) components and a trend component.

The empirical orthogonal function (EOF) is utilized to extract the dominant spatial pattern according to the leading mode of the anomalies in moisture sources distribution. North statistical testing (North et al. 1982) is applied to determine the significance of the EOF modes. Correlation and composite analyses are performed to diagnose relationships between precipitation and large-scale climate features. Linear regression is used to explore the linear trends. The Student's t-test is used to examine the significance of the linear trend.

3 Results

3.1 Decadal shift of summer precipitation

Here, the TRH is geographically defined as a rectangle region, with latitude and longitude ranging from 31.25°N to 37.25°N and 89.25°E to 102.75°E (Fig. 1). This definition is similar to previous studies (e.g., Sun et al., 2018, 2020; Zhang et al. 2019a), but differs from that in Liu et al. (2023). As shown in the top panel of Fig. 2a, the precipitation in the TRH is characterized by a strong annual cycle for the summer season. To determine the decadal regime shift, we decompose the time series of regional annual precipitation

into several Intrinsic Mode Function (IMF) components with the EEMD analysis method (Fig. 2a). Obviously, the regional precipitation over the TRH is featured by a variation on multiple temporal scales. More importantly, the long-term trend of summer precipitation is characterized by two distinct periods (1980–1995 and 1996–2017), corresponding to a decreasing trend and an increasing trend, respectively, which indicate a turn-point around 1995/1996 (as shown in Fig. 2b with Mann-Kendall trend test). The change point around 1995 is similar to the study by Li et al. (2022). The difference between two studies could be partly attributed to the difference in target region selection and the definition used.

According to the above analysis, the dry and wet period is defined as P1 (1980–1995) and P2 (1996–2017), respectively. Figure 2c presents the spatial distribution of differences in summer precipitation between the two periods (P2–P1). It is easy to find that the increased rainfall overwhelms the whole region after the 1995 shift. Quantitative evaluation shows that there is 17.9% more precipitation (274.29 versus 286.43 mm) in the wet period (1980–1995) than in the dry period (1996–2017). Although a broad area of the THR region receives more precipitation compared to the wet decadal period, the decadal signal is not geographically homogeneous but varies from above 28 mm (increased) in the northwest to less than 28 mm (decreased) in the southeast (Fig. 2c). These northwestern positive values and southeastern negative values over the TRH coincide with the drying tendency over the southern slope of the TP (Wang et al. 2022b) and the wetting tendency over the inner TP (Sun et al. 2020), respectively.

3.2 Relationship between changes in moisture sources and precipitation

The main objective of this study is to examine the causes on the dry-to-wet shift from the perspective of moisture changes. So it is a priority to answer the question: How much do the changes in moisture sources reflect the dry-to-wet transition in precipitation in the TRH region? To this end, based on the large ensemble of Lagrangian backward tracking and E-P diagnosis, we examine the time series of the regional moisture sources contribution and summer precipitation for the period of 1980–2017. As shown in Fig. 3, the annual variations in region-averaged summer mean precipitation in the TRH region correspond well with the variations in moisture sources contribution. The Pearson correlation coefficient reaches +0.47, which is statistically significant at the 95% confidence interval. Quantitative evaluation also exhibits that the magnitudes of regional precipitation and moisture source are similar.

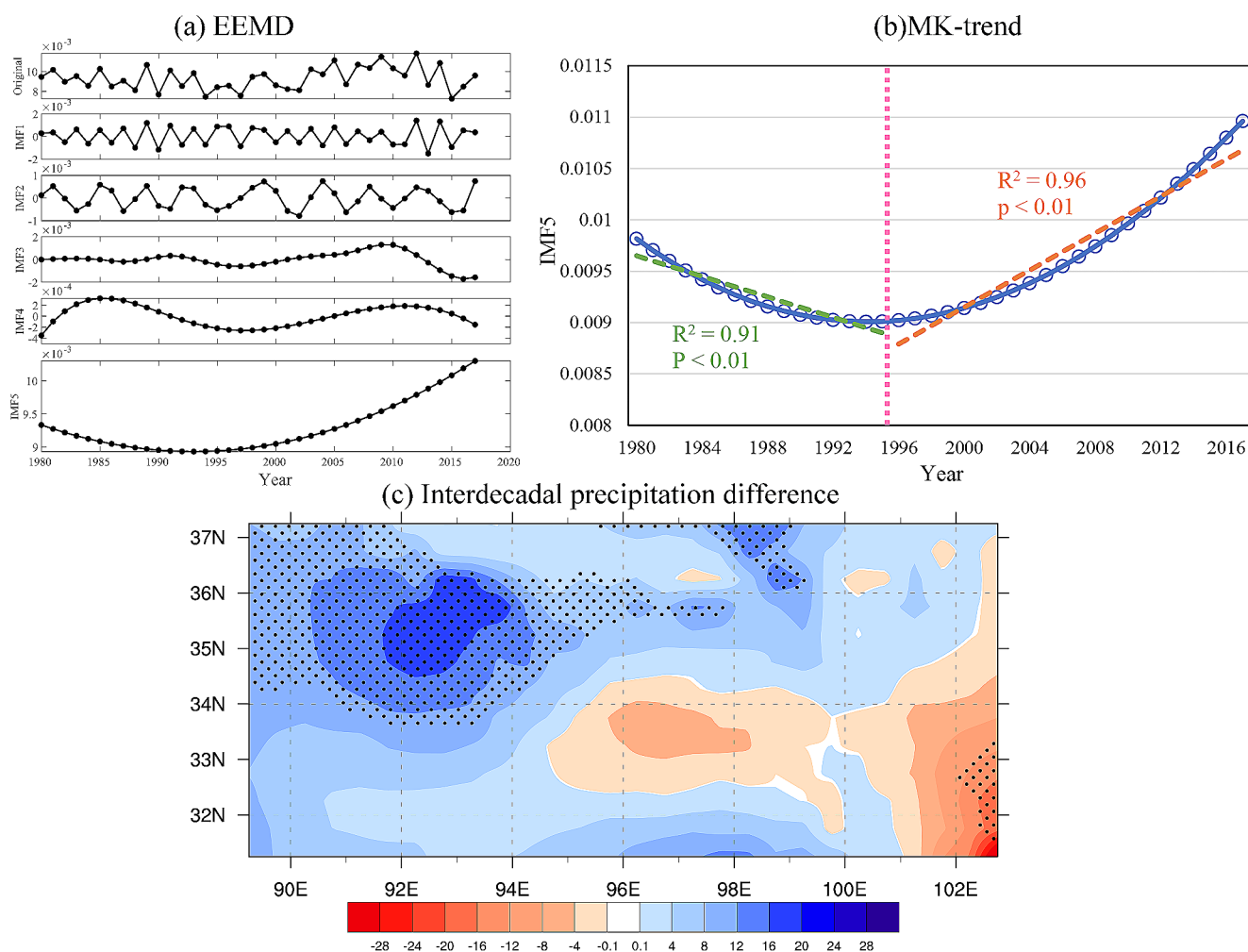


Fig. 2 (a) EEMD of the TRH region regional mean precipitation series in summer season for the period of 1980–2017. (b) Mann-Kendall trend test for IMF1-IMF5. (c) Composite maps of summer precipitation differences (shadings, units: mm) between dry and wet periods

(P2-P1). Here, the dry period 1980–1995 (P1) and dry period 1996–2017 (P2) are defined as in text. The value $P < 0.01$ in (b) and stippling in (c), respectively, indicates the difference is statistically significant at the 95% confidence level

To further examine the relationship on the decadal scale, the two time series above are smoothed with a 9-year running mean method. The correlation coefficient for the regional precipitation and moisture sources reaches 0.9, which is statistically significant at the 99% confidence interval. This strong correlation efficient implies that, on the one hand, the decadal variation in regional precipitation in TRH region is closely linked with the changes in moisture sources. Considering that the moisture sources serve as the main component of water cycle and an essential prerequisite of precipitation, this result, on the other hand, indicates the feasibility to explore the causes of dry-to-wet transition from the perspective of changes in moisture sources, which in turn supports the robustness of the moisture sources identification method used in this study.

The water vapor transport of precipitation events is rather complicated due to the involvement of multiple time scales

ranging from several hours to a few days. To take a closer look at the relationship between the moisture changes and the summer precipitation over the TRH, we conduct a conventional EOF analysis for the moisture sources with specific backward tracking days. The patterns of the first two EOFs of (E-P)₁₋₂, (E-P)₃₋₆, and (E-P)₇₋₁₀ are displayed in Fig. 4. For (E-P)₁₋₂, EOF1 represents a north-south dipole structure with low values in the north and east of the study area and high values located at the southwestern TP, while EOF2 shows a three-pole pattern characterized by low values throughout most of western TP and significantly high values distributed over the northeastern TP and part of Indian subcontinent. The first two EOFs of (E-P)₁₋₂ together explain 41.7% of the variance, and EOF1 alone explains 25%. The pattern of EOF1 (EOF2) reflects the meridional (southwest-northeast direction) variation, which is obviously related to the strength of Southern Asian summer monsoon. With

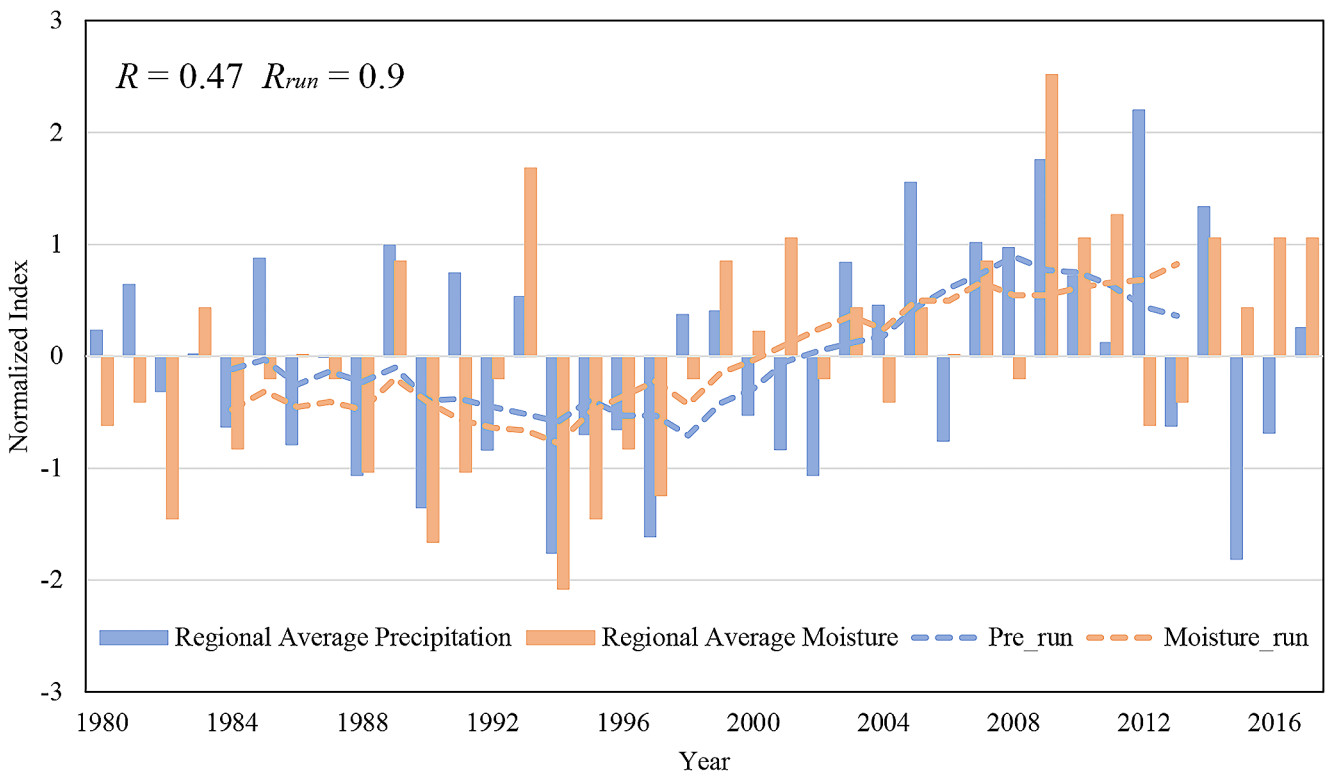


Fig. 3 Time series of regional summer mean precipitation (blue) and diagnosed moisture sources contribution (red) during the period of 1980–2017. The dashed line indicates the decadal signal with 9-year running mean. The correlation coefficients (after 9-year running mean)

between the precipitation and moisture contribution are labeled in the upper-left corner, with a significant level exceeding 95% (99%) significant level

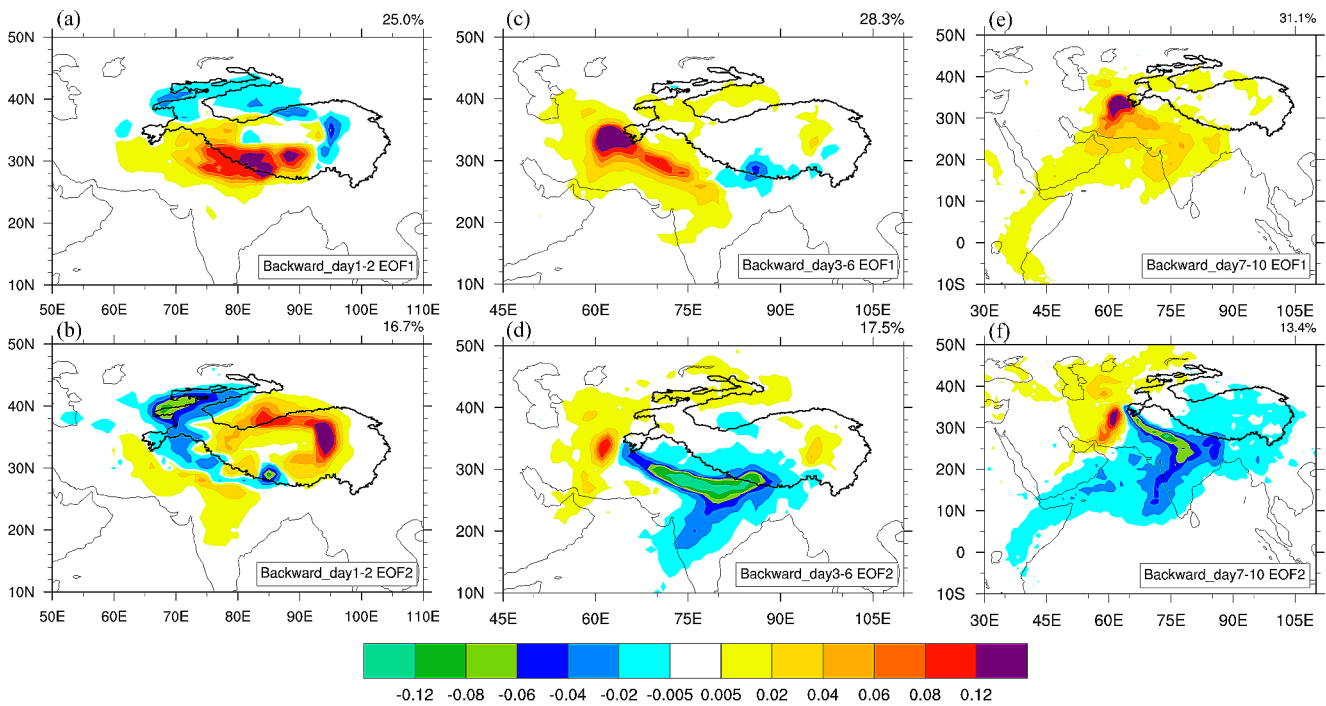


Fig. 4 The first leading modes EOF1 (a, c, e) and second modes EOF2 (b, d, f) generated from the conventional EOF decomposition of moisture sources contribution (1980–2017) in the TRH region for

the $(E-P)_{1-2}$ (a, b), $(E-P)_{3-6}$ (c, d), and $(E-P)_{7-10}$ (e, f). The variance explained by the corresponding modes is labeled in the upper-right corner of each plot

respect of the $(E-P)_{3-6}$, and $(E-P)_{7-10}$, EOF1 shows simple mode, namely, almost the same high values in the whole area, indicating that the EOF1 is dominated by the long-term dry-to-wet trend, and EOF2 manifests a northwest-southeast dipole structure, which is potentially modulated by the combined influence of the South Asian monsoon and the westerlies (Liu et al. 2023; Wang et al. 2023).

What are the time scales of the moisture sources transport most relevant to the dry-to-wet shift in precipitation in the TRH region? To answer this question, we examine the correlation between time series of principal component (PC) with the regional summer precipitation. The time series being smoothed by the 9-year running mean are presented in Fig. 5. It is surprising to find that the temporal variation of PC1 for the $(E-P)_{1-2}$, $(E-P)_{3-6}$, and $(E-P)_{7-10}$ shows a transition from the negative to positive phase, all closely related to the regional summer mean precipitation.

The correlation coefficients among them are 0.62, 0.54 and 0.92, respectively, all of which are statistically significant at 95% confidence level. Although the relationship between the time series of PC2 and precipitation varies, these results imply that the dry-to-wet shift in summer precipitation in TRH is regulated by the changes in moisture sources across multiple transport time scales.

3.3 Moisture sources changes associated with the dry-to-wet shift

Figure 6 presents the spatial distribution of summer moisture sources that contributed to the precipitation in the TRH region for the period P1 (Fig. 6a) and P2 (Fig. 6b), and their differences (P2-P1). For the period of P1 and P2, the summer climatic state of moisture sources exhibits a similar spatial pattern with an overall southwest-northeast distribution,

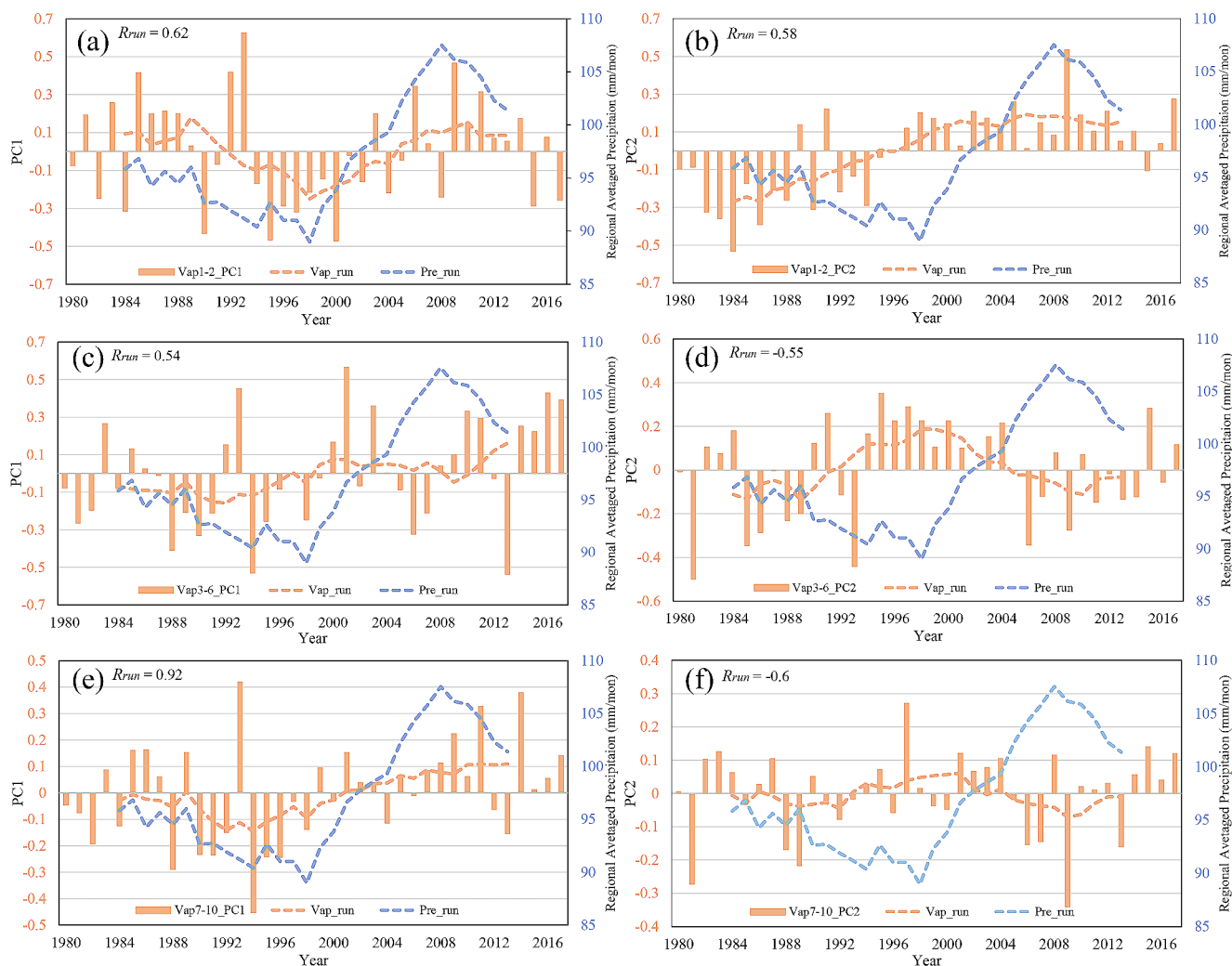


Fig. 5 The time series of principal component (PC) of the first leading modes EOF1 (a, c, e) and second modes (b, d, f) of $(E-P)_{1-2}$ (a, b), $(E-P)_{3-6}$ (c, d), and $(E-P)_{7-10}$ (e, f) obtained by EOF analysis of total moisture sources contribution in the TRH region. The dashed blue and

orange line represented the decadal signal of precipitation and moisture sources contribution after 9-year running mean, respectively. The correlation coefficients for the PC and precipitation are labeled in the upper-left corner of panel

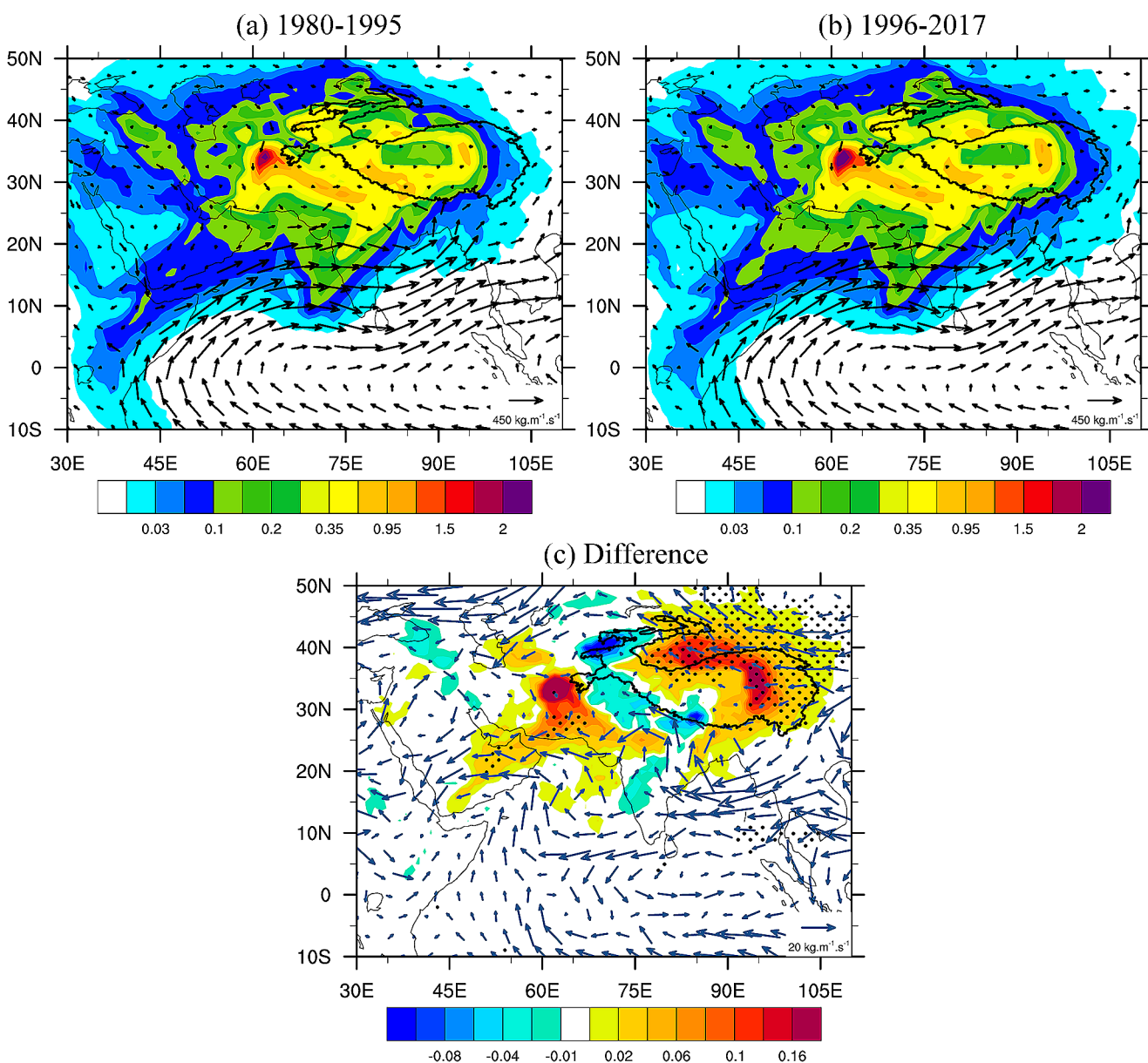


Fig. 6 Spatial distribution of summer moisture sources contributed to the precipitation in the TRH region (color shaded, *mm/day*) for the period of P1 (a) and P2 (b), together with their difference (c). The vector represents the vertical integrated water vapor flux (unit in

kg · m⁻¹ · s⁻¹). The dotted area in (c) indicates the difference is statistically significant at the 95% confidence level. P1 (1980–1995) and P2 (1996–2020) are defined as in text

which is consistent with the direction of the vertically integrated water vapor flux in the Eulerian framework. The moisture sources cover a vast region, including the Bay of Bengal, the Arabian Sea and even the Indian Ocean to the south, the entire Tibetan plateau, and the parts of Central Asia to the northwest. Overall, it can be found that, although the summer water vapor transport of the TRH region seems to be dominated by the combined influence of the South Asian monsoon and the westerlies (Liu et al. 2023; Wang et al. 2023), the evaporation and recycling processes make a larger contribution to the precipitation.

Compared with the summer climatic state of moisture sources, the spatial distribution of changes in moisture sources between the P1 and P2 (P2-P1, shown in Fig. 6c) covers relatively smaller areas. It is noteworthy that there are two prominent positive-value centers of moisture sources: one is located to the southwestern side of the TP, and the other is concentrated over the northeastern TP itself. Based on the evaluation of their geographical locations, the former implies the dominance of the Indian summer monsoon in regulating water vapor transport for the precipitation in the TRH, while the latter implies the role of evaporation

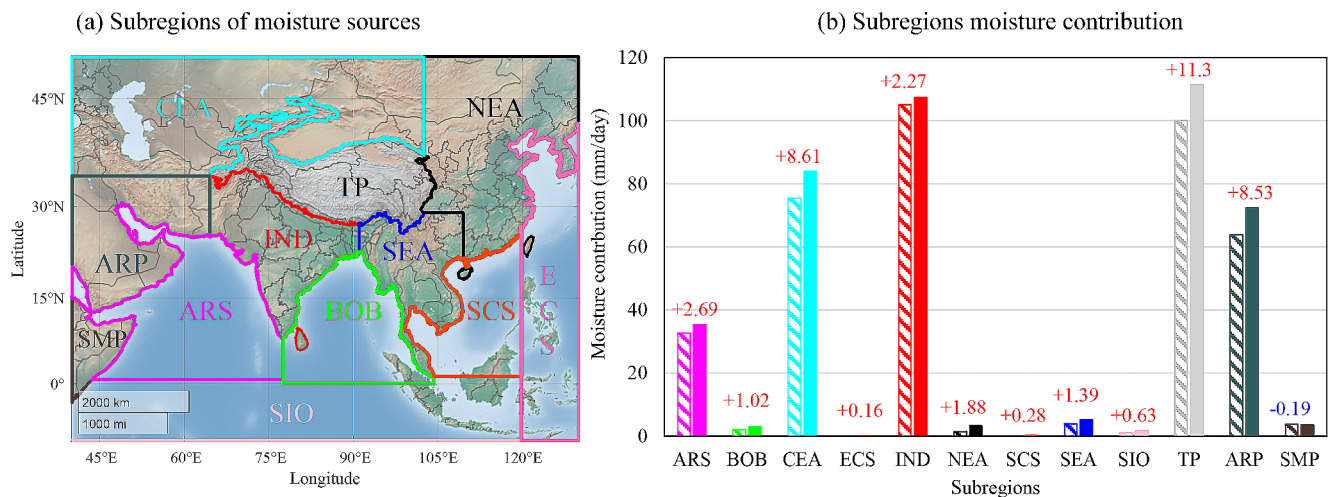


Fig. 7 (a) The geographical location of 12 sub-regions for the Arabian Sea (ARS), Arabian Peninsula (ARP), Bay of Bengal (BOB), Central Eastern Asian(CEA), Eastern China Sea(ECS), Indian continent(IND), Northeastern Asian(NEA), Southern China Sea(SCS), Southeastern Asian(SEA), South Indian Ocean(SIO), Somali Peninsula (SMP),

Tibetan Plateau(TP). (b) Moisture contribution (mm/day , the colors of the bars in the figure match the colors of subregions to TRH region summer precipitation in P1 (solid color fills) and P2 (pattern fills), and the values in red and blue represent specific differences in interdecadal moisture contributions

Table 1 Ratios of relative moisture contribution by individual subregions during P1 and P2 and their corresponding differences (P2-P1)

Percentage(%)	ARS	BOB	CEA	ECS	IND	NEA
P1	8.37	0.52	19.35	0.04	26.96	0.37
P2	8.25	0.71	19.62	0.07	25.06	0.77
Difference	-0.12	0.19	0.27	0.03	-1.9	0.41
Percentage(%)	SCS	SEA	SIO	TP	ARP	SMP
P1	0.09	1	0.28	25.67	16.38	0.96
P2	0.14	1.24	0.4	26	16.9	0.83
Difference	0.06	0.23	0.12	0.33	0.52	-0.13

or local precipitation circulation processes in the TP and its surrounding regions in contributing notably to the increased precipitation in the TRH. Recently, Li et al. (2022) pointed out the precipitation recycling ratio showed an increasing trend. The enhancement of South Asian summer monsoon was reported by Rai and Raveh-Rubin (2023) as well.

For an in-depth quantitative evaluation, we divide the whole Asian region into twelve sub-regions to quantify the contribution of individual source areas, namely, for the Arabian Sea (ARS), Arabian Peninsula (ARP), Bay of Bengal (BOB), Central Eastern Asian (CEA), Eastern China Sea (ECS), Indian continent (IND), Northeastern Asian (NEA), South China Sea (SCS), Southeastern Asian (SEA), South Indian Ocean (SIO), Somali Peninsula (SMP), and Tibetan Plateau (TP) (as shown in Fig. 7a). It can be observed that, comparing to the P1 period, the moisture contribution increases during the P2 period in almost all subregions except the Somali Peninsula (SMP). Although the Indian continent (IND, 26.96%), Tibetan Plateau (TP, 25.67%), Central Eastern Asian (CEA, 19.35%) and Arabian Sea (ARS, 8.37%) serve as the main moisture contributors to the summer precipitation, their roles in modulating the

dry-to-wet shift differ from each other. Among them, the Plateau region (TP) including the TRH region itself, the Central Eastern Asian region (CEA), and the Arabian Peninsula (ARP) rank as the three leading contributors to the enhanced moisture supply, with the accumulated moisture sources on all grids increased by 11.3, 8.61 and 8.53 $mm \cdot year^{-1}$, respectively. The increase in water vapor contribution by the terrestrial regions is much larger than that by the oceanic (grid accumulated moisture change: +33.79 versus +4.78 mm).

To further examine the relative importance of different subregions in regulating the precipitation, we compare the ratios of relative contribution by the subregions during two periods (Table 1). In contrast to these regions, those terrestrial regions, in particular the NEA (+0.41%), the TP (+0.33%), the CEA (+0.27%), and the ARP (+0.52%), are the regions with the largest increase in relative contribution. These results imply that, even though the absolute contribution from the moisture source dominated by the South Asian monsoon increases, it plays a relatively minor role in regulating the decadal variability in summer precipitation. On the contrary, those terrestrial source regions with

the evaporation or precipitation recycling could exert strong impacts on the dry-to-wet shift.

To discern the dependence of the dry-to-wet shift in summer precipitation on the moisture sources evolution with multiple transport time scales, we calculate the contributions of individual sub-source area to the regional moisture changes on specific backward tracking 1–10 days (Fig. 8a), as well as their accumulated contributions (Fig. 8b). As seen from Fig. 8, the increased moisture contributions over the TP and ARP with the transport time scale less than 4 days are more significant, further affirming the vital roles of these two regions in dominating the dry-to-wet transition of summer precipitation in the TRH region. The results show that the contribution by the individual region to the increased summer rainfall between the P1 and P2 shows a dependency on the time scales of backward tracking. More specifically, the significant contributions by the TP and CEA region remain steady during the 10-days backward tracking, although they show a slight decrease and increase with tracking time elapsed, respectively. On the contrary, the contribution from other regions varies in line with the backward tracking days. For instance, the IND and ARP show an abrupt increase around 2–3 days, largely due to their distance from the target region. The accumulative contribution confirms the dominant role of the enhanced moisture sources from the NEA, the TP, the CEA in regulating the dry-to-wet shift in the TRH region.

3.4 Linkage to atmospheric conditions

Commonly, the anomalies of atmospheric circulations and sea surface temperature (SST) are considered as two prominent factors in modulating the regional precipitation. Sun and wang (2018) have demonstrated that anomalous wave trains significantly influence the decadal variability of the summer precipitation in the TRH region. It is also reported that the precipitation in the southern TP and Northwest

China is associated with changes of SST over the equatorial central Pacific and the Indo-Pacific warm pool (Zhou et al. 2019; Yue et al. 2021; Shang et al., 2022; Wang et al. 2022b). Comparing to the P1 period, the atmospheric circulations and sea surface temperature shows an anomalous feature during the P2. The difference of the 500-hPa geopotential height between P1 and P2 appears a structure of anomalous wave trains between the $30^{\circ}N - 60^{\circ}N$ (Fig. 9a). In particular, the anomalous anticyclonic system over the northeastern TP, on the one hand, enables more air mass to enter into the northeastern TP, conveying more moisture to the TRH region from higher latitudinal areas and the East China. On the other hand, the easterly winds at the surface of the anticyclone also inhibit the outflow of water vapor from the eastern boundary of the TP. For the SST differences, the SST warming is almost found throughout the whole region during the P2 period, with high values covering the Arabian Sea-Indian Ocean and the Indo-Pacific warm pool (Fig. 9b). The warming over these distant oceanic regions is likely to accelerate the water cycle process and thereby enhance the long-distance water vapor transport, suggesting that the oceanic region could act as an additional moisture source for the decadal shift of summer precipitation in the TRH region.

For a better understanding the relationship between the anomalous circulation and dry-to-wet shift of summer precipitation over the TRH region, we firstly derived three atmospheric indices as mentioned above, i.e., the SRI, (Fig. 10a), the WPI, (Fig. 10b), and the PDO (Fig. 10c), based on the EOF1 for the variations of mean wind (Fig. 10d) and the strength of SST anomalies over the Indo-Pacific Warm Pool (Fig. 10e) and the North Pacific basin (Fig. 10f). As seen from Fig. 10a and b, the time series of SRI and WPI are both characterized by a decadal transition around the middle of 1990s, which is agree with the variation of summer mean precipitation. But the PDO index (Fig. 10c) shows a different trend. Regressions of summer precipitation anomalies against the SRI and WPI in the TRH region during the

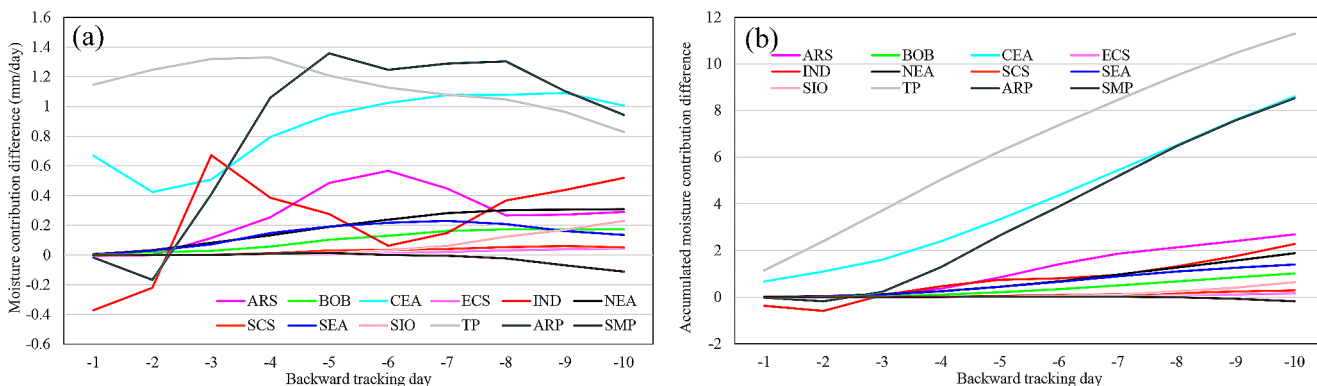
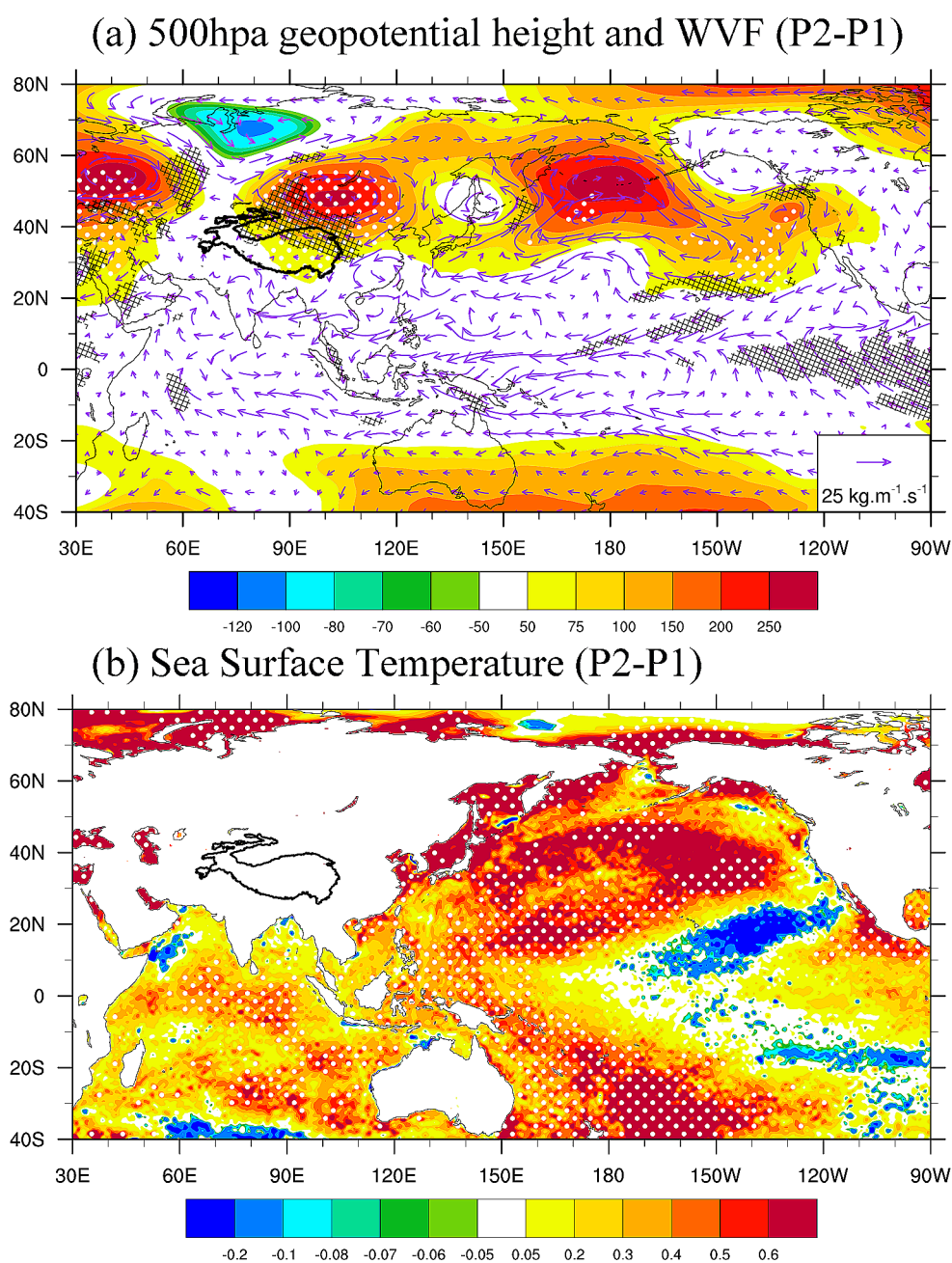


Fig. 8 Quantitative contributions of individual sub-source regions of moisture sources on specific backward tracking day (1–10 d) to the regional moisture sources changes (P2-P1) in the TRH region (a),

and their corresponding cumulative contribution (b). The individual demarked sub-regions are defined same as in Fig. 7

Fig. 9 Differences of (a) 500-hPa geopotential height (shaded, $m^2 \cdot s^{-2}$), vertically integrated water vapor flux (vector, $kg \cdot m^{-1} \cdot s^{-1}$), and (b) sea surface temperature (shaded, $^{\circ}C$) between P1 and P2 (P2-P1). The black grids in (a) and dotted areas in (b) means the difference is statistically significant at the 95% confidence level



1980–2017 are exhibited in Fig. 10g and h, respectively. It can be found that, both for the SRI and WPI, the spatial pattern of precipitation anomalies highly resemble that of decadal changes in precipitation as shown in Fig. 2c, with the positive values distributed over the northwest of the TRH and the negative values over the southeastern TRH. This resemblance suggests that the variation in SRI and WPI is closely correlation to the changes in summer precipitation over the TRH region. Although the anomalies in regressed summer precipitation by the PDO index (Fig. 10i) is distinct differ from that of the SRI and WPI, the region of significant positive values is overlapped with that increased

precipitation, indicating that the PDO variation is also likely to contribute to the dry-to-wet transition in summer rainfall over TRH region.

To further illustrate the impacts of the indices on the process of water vapor transport straightforwardly, we calculated the difference in regressed summer moisture sources contribution to the TRH region against the SRI, WPI, and PDO between the P1 and P2 period (P2-P1) (Fig. 11). The results evidenced that, under the modulation of the three indices, the enhanced moisture source covered vast regions, in particularly over the terrestrial northeastern TP. Additionally, the decadal changes in SRI and WPI can lead to more

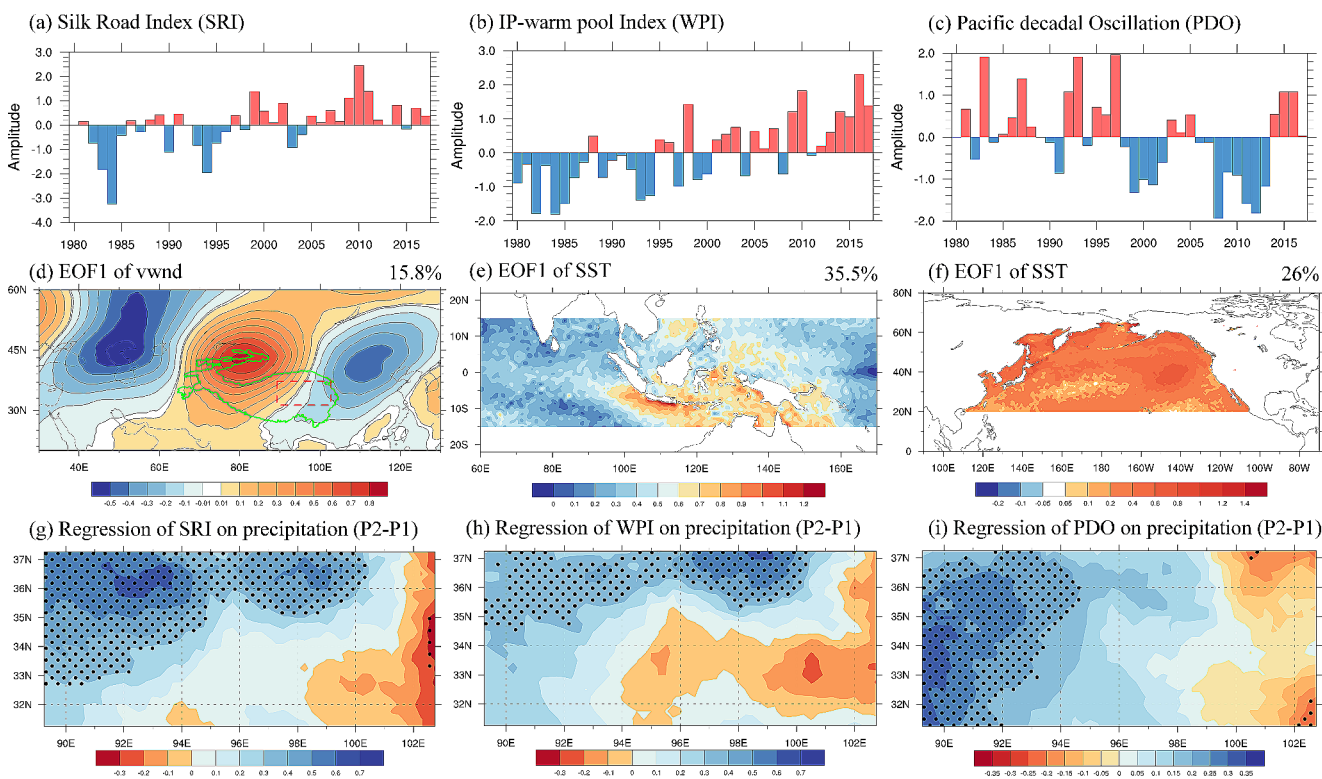


Fig. 10 Time series for (a) the Silk Road index (SRI), (b) the Indo-Pacific Warm Pool Index (WPI) and (c) the Pacific Decadal Oscillation (PDO) index. (d) EOF1 of mean meridional wind during summer season, in which the solid green line indicates the location of Tibetan Plateau and the dashed rectangular box represent the TRH region. The

EOF1 of SST over warm pool region and over North Pacific basin is represented in (e) and (f), respectively. (g), (h), and (i) shows the regressions of summer precipitation anomalies against the SRI, WPI, PDO respectively (unit in mm, regions exceeding the 95% significance level are dotted)

water vapor supplies from long-distance lower latitudinal and the oceanic regions to the TRH region. The SRI and WPI index are highly correlated to the regional integrated moisture source change during the period of 1980–2017, with the coefficients reaching 0.93 and 0.9, respectively, both of which are statistically significant at the 99% confidence level. These results demonstrate that the anomalous atmospheric circulation and SST could contribute to the dry-to-wet changes in summer precipitation over the TRH region via its modulation on the moisture source contribution.

Why the changes in the Silk Road Pattern (SRP) and the SST from P1 to P2 could potentially account for the dry-to-wet shift in summer precipitation over the TRH region? To answer this question, we further explore its underlying mechanisms from the perspective of its impacts on the atmospheric circulation. Firstly, we show the spatial distribution of difference in anomalies of 500-hPa zonal and meridional wind between the P1 and P2 period in the Fig. 12a and b, respectively. Comparing to the P1, the anomalies in zonal wind exhibit a wave train-like structure at 500-hPa level during P2 period (Fig. 12a), and these anomalies are extending nearly from the surface to the upper troposphere (Figure not shown). Especially, the obvious easterly wind anomalies

occurred to and over the northeastern TP, which could result in the decreases in westerly and thereby maintain the air mass or water vapor retaining over the TRH region for a longer time. This change in zonal wind partly explains the reason why the moisture source contribution from the local recycling processes enhanced during P2 period. A noteworthy southerly wind anomaly exists simultaneously over the western TP, ranging from the oceanic to the higher latitudinal areas (Fig. 12b). This meridional wind anomaly is likely linked to anomalous strong southwesterly winds in the southern upstream region (Yang et al., 2024). Hence, significant wind anomalies prevail over and to the northeastern TP, and the southwestern TP is under the control of peripheral southwesterly airflows of the anomalous anticyclonic circulation. Such atmospheric circulation anomalies can affect the water vapor transport into TRH region, resulting in more precipitation over this region.

To examine the association of anomalous SST with the changes in atmospheric circulation, Fig. 12c-d and e-f shows the anomalies in the 500-hPa horizontal winds regressed against the WPI and PDO index for the P1 and the P2 period, respectively. As seen from these figures, the anomalies in wind anomalies explained by the decadal changes in the

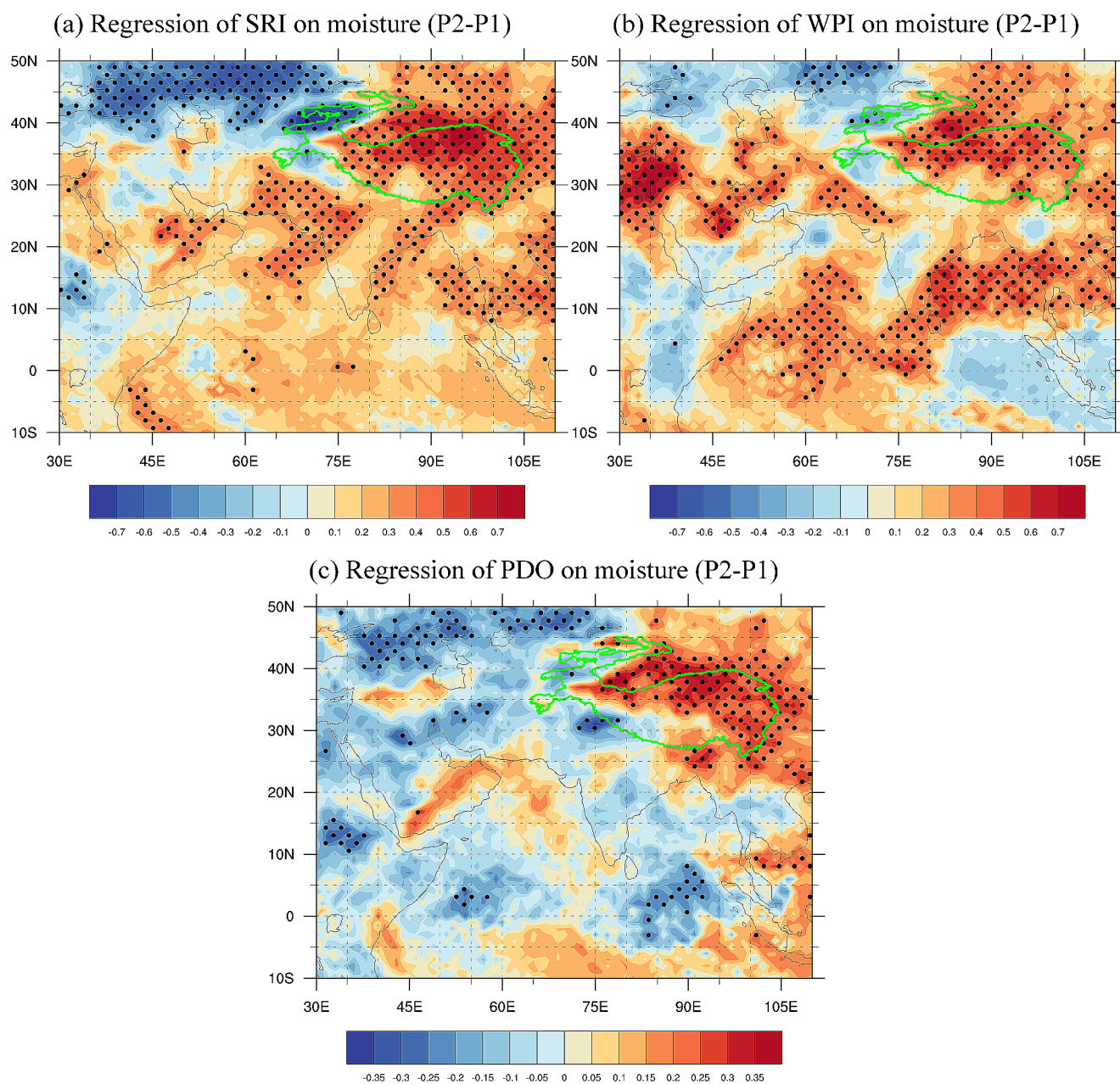


Fig. 11 Difference in regressed summer moisture source contribution to the TRH region against the (a) SRI, (b) WPI, and (c) PDO between P1 and P2 (P2-P1). The dotted area indicates the difference is statistically significant at the 95% confidence level

WPI and PDO index is particularly featured by an easterly wind anomaly over the northeastern TP and southerly wind anomaly around the western TP, which largely resemble to that shown in Fig. 12a and b. These results suggest that the SST in the Indo-Pacific warm pool and the North Pacific could modulate the atmospheric circulation via altering the wind fields, thereby exerting an impact on the anomalous transport of water vapor.

Regarding to the impacts of SRI index, we provide the spatial pattern of the SRP during the P1 and P2 period (Fig. 13). Note that here the Silk Road Index is defined as

the EOF1 of summer meridional wind on 200-hPa level. It can be found that the spatial pattern of SRP shows a remarkable contrast between P1 and P2. Specifically, the distribution of the SRP over the TRH is in its positive phase for P1, while it changed into a negative phase for P2. This negative phase is beneficial for the increase in summer precipitation over the TRH region. The difference in regressed 500-hPa geopotential height against the SRI between the P1 and P2 (Figure not shown here) shows that the decadal shift in meridional wind anomaly is linked to anomalous cyclonic (anticyclonic) circulation in the western (eastern) part of

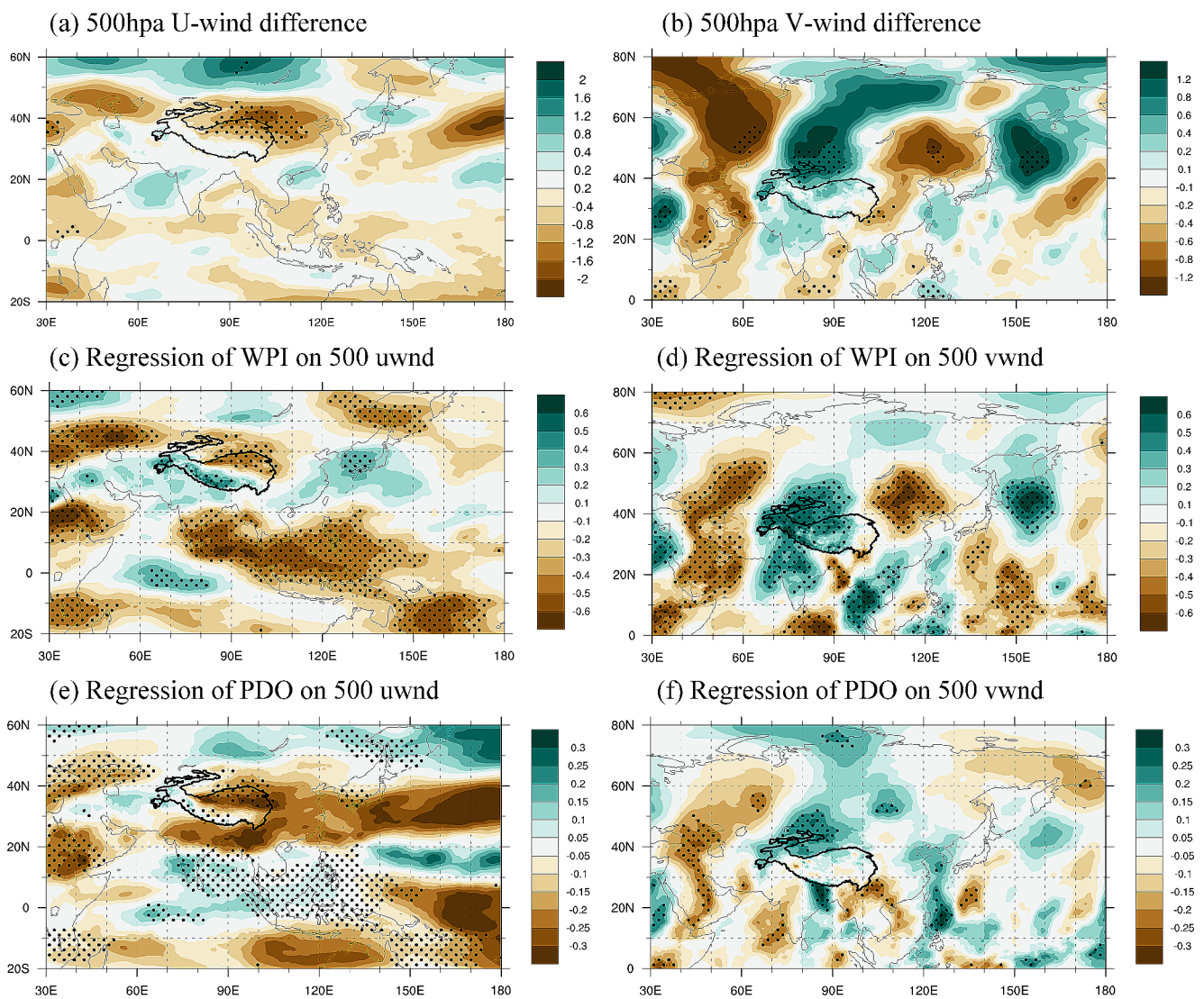


Fig. 12 The spatial distribution of difference in zonal (a) and meridional (b) wind between the P1 and P2 period (P2-P1) on 500-hPa height, together with their regressed winds against the WPI (c, d) and PDO (e,

f) index. The dotted area indicates the difference is statistically significant at the 95% confidence level

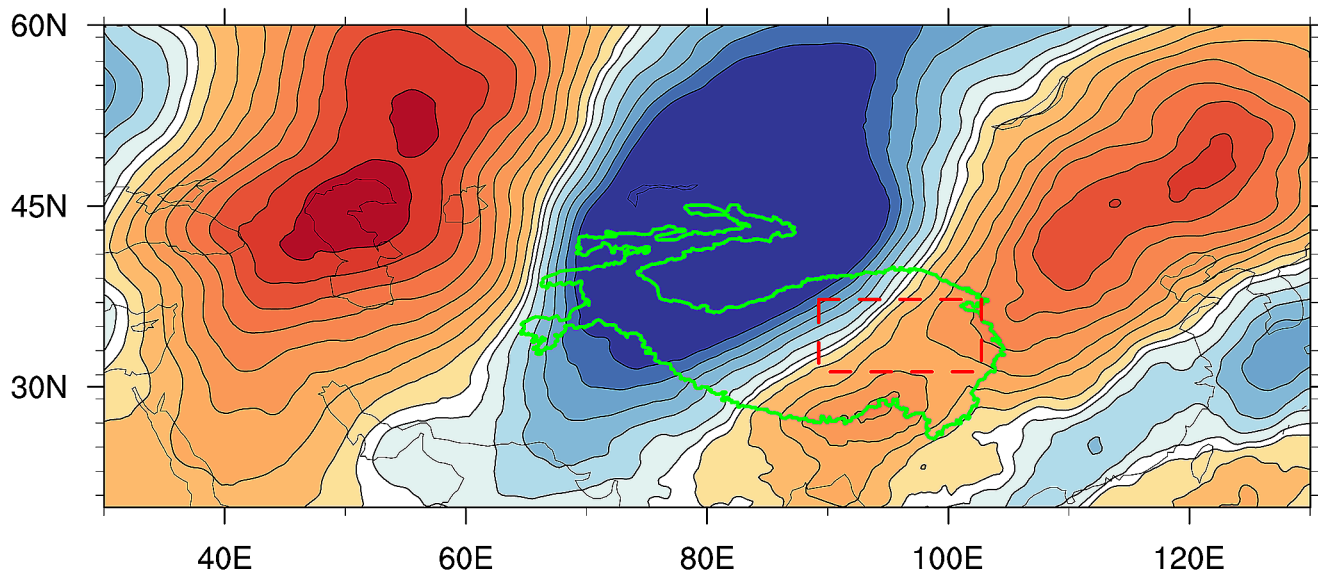
northern Tibetan Plateau. This anomalous circulation pattern is obviously benefits for the strong southwesterly winds in the southern upstream region and anomalous weak westerly winds in the northern upstream region of the TP. This result is supported by a more recent study by Sun et al. (2024), in which they argued that the inter-annual variation of the precipitation on the Tibetan Plateau is closely related to the changes in meridional wind, and the southerly wind anomalies would result in more precipitation in the northern TP.

4 Discussion

4.1 Comparison with previous studies

Under a changing climate, the atmospheric water cycle processes over the TRH region have been greatly enhanced (Wang et al. 2023), along with a dry-to-wet transition in summer precipitation over this region. Despite the widespread interest of scientific community, the causes of such climate shifts are still not well understood. On the one hand, for the external forcing, previous studies assumed that the weakening of the westerlies could make it more convenient for water vapor to be trapped over the TP, leading to an increase in the moisture contribution from the TP and Northeast China (Jiang et al. 2023). The interdecadal shift

(a) Meridional wind for P1(1980-1995)



(b) Meridional wind for P2(1996-2017)

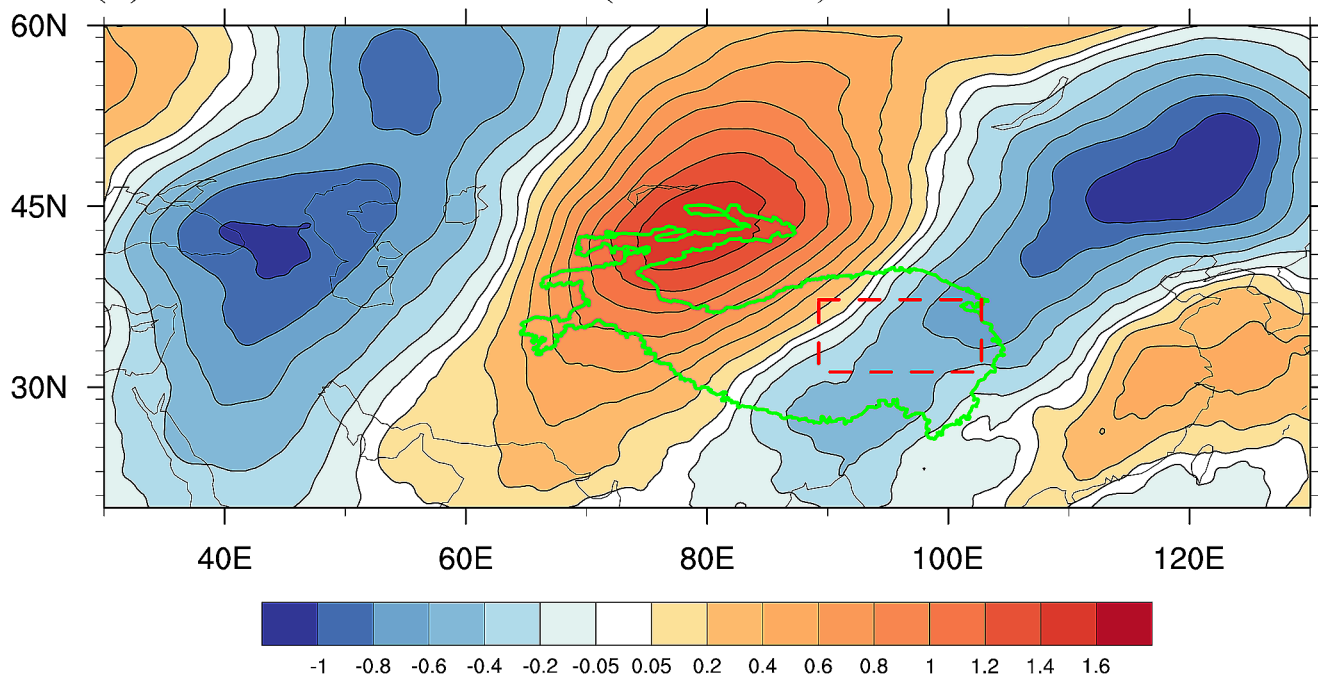


Fig. 13 The spatial pattern for the composite meridional wind for the P1 and P2 period, derived from EOF analysis

of summer precipitation in the TRH region is likely to correspond to the strengthening of the South Asian summer monsoon and the relatively weakening of the westerlies (Sun et al. 2020). More recently, Liu et al. (2023) have shown that the external forcing tied to the increased southerly and easterly water vapor transport made a significant contribution to the dry-to-wet transition over the TRH region. On the other hand, a large number of previous studies have demonstrated

the strengthened local recycling over most parts of the TP (Curio et al. 2015; He et al. 2021; Li et al. 2022). More specifically, He et al. (2021) argued that the dominant increasing water vapor over the western TP is dominated by the internal cycle of the water cycle, which is largely related to the enhanced precipitation recycling (Li et al. 2022; Guo et al. 2022).

Here we have conducted an analysis of decadal changes in the moisture sources for the water vapor reaching the TRH region during the summer season for the period of 1980–2017, with particular focus on the causes of the dry-to-wet shift in the summer precipitation between periods 1980–1995 and 1996–2017. The results of this study highlight the enhanced contribution by the terrestrial sources to the dry-to-wet shift in the TRH, which are largely tied to the processes of land evaporation or precipitation recycling process.

Regarding the relative importance of different moisture sources, the results presented herein have shown that the terrestrial sources play a leading role in modulating the dry-to-wet shift, since their contributions is several times higher than that by the oceanic sources. This result seems slightly different from recent studies. For instance, Wang et al. (2022b) argued that the dry/wet variations could be attributed to the enhancement in Indian Ocean sea surface temperature. Here, there is a caveat that should be pointed out first. As to the moisture sources identification method of this study, we diagnose the variable of evaporation minus precipitation (E-P), rather than the evaporation itself. Considering the large amount of precipitation occurred over the oceanic region, the moisture contribution to the precipitation by parts of oceanic regions could not be examined directly. In this sense, the results presented herein do not disagree with those previous studies.

4.2 Uncertainties of this study

The robustness of the results presented in this study largely depends on the accuracies of methods used to identify the moisture source. Although the large uncertainty is inhibited in the Lagrangian modeling and moisture sources diagnosis (Gimeno 2020), the relatively high spatiotemporal resolution and relatively high performance over the TP for the ERA-Interim reanalysis (Gao et al. 2014) has documented the accuracy of the trajectory calculation. More importantly, the analysis of this study is mainly based on the comparison of moisture source between the P1 (1980–1995) and P2 (1996–2017), which, to a large extent, weakens the impact of absolute errors in the ERA-Interim reanalysis. Additionally, the close relationship between the diagnosed moisture sources and the precipitation during the summer season evidences the robustness of the study.

Another caveat should be kept in mind. The method of E-P diagnosis used in this study can not provide exact details on the local recycling. Considering that the distinctly physical processes are sensitive to the transport time scale for the vapor reaching the TRH, the examination on the dependency of moisture sources on the transport time scales could shed light on these issues. Figure 7 provides

the distributions of differences in moisture sources between P1 and P2 in terms of different transport time scales on specific days. The results show that the discrepancy of moisture sources between the P1 and P2 varies spatially in line with the transport time elapsed. For relatively short-term (1–2 days) water vapor transport, the increased moisture sources are confined to a limited region, with the most significant positive values centered on the east and north of TP and negative values to and over the western TP. Along with the backward tracking time elapsed, the regions of increased moisture uptake are enlarged. For backward tracking of 3–6 days, the regions with positive values are strengthened northeastward beyond the northern TP and southwestward to the Iranian plateau, the ARS and ARP, respectively. For a longer period of 7–10 days, except the parts of IND and SMP, the whole region is featured by the positive contribution, and the increased moisture could be tracked back to the far oceanic areas, even the moisture transport crossing the equator from the south hemisphere. It is worthy to note that only the eastern and northern TP act as a steady positive contributor with difference statistically significant at the 95% confidence level (Fig. 14), indicating that local recycling processes on the TP and its adjacent regions contribute remarkably to the interdecadal increase of summer precipitation in the TRH region.

5 Summary and conclusions

The Three-Rivers Headwater (TRH) region is an important reservoir of freshwater resources in China. Under a changing climate, the precipitation over this region has been altered as well. Building on the gauged precipitation data and statistical analysis, we detected a dry-to-wet shift in summer precipitation over the TRH region around 1995/1996. With the 38-year high resolution Lagrangian modeling and a relatively sophisticated moisture sources diagnosis, the spatiotemporal characteristics of changes in moisture sources accompanying with the dry-to-wet transition are explored, particularly aiming to reveal the underlying mechanisms of decadal transition in summer rainfall. The main conclusions of this study could be summarized as follows:

- 1) The summer precipitation in the TRH region is featured by a dry-to-wet transition from period of 1996–2017 to 1980–1995. The variability of moisture sources for the water vapor reaching the TRH region are closely linked to the regional summer precipitation in the TRH region. This relationship remains steady across multiple transport time scales associated with the water vapor.
- 2) The dry-to-wet shift in summer precipitation in TRH is regulated by the changes in moisture sources across

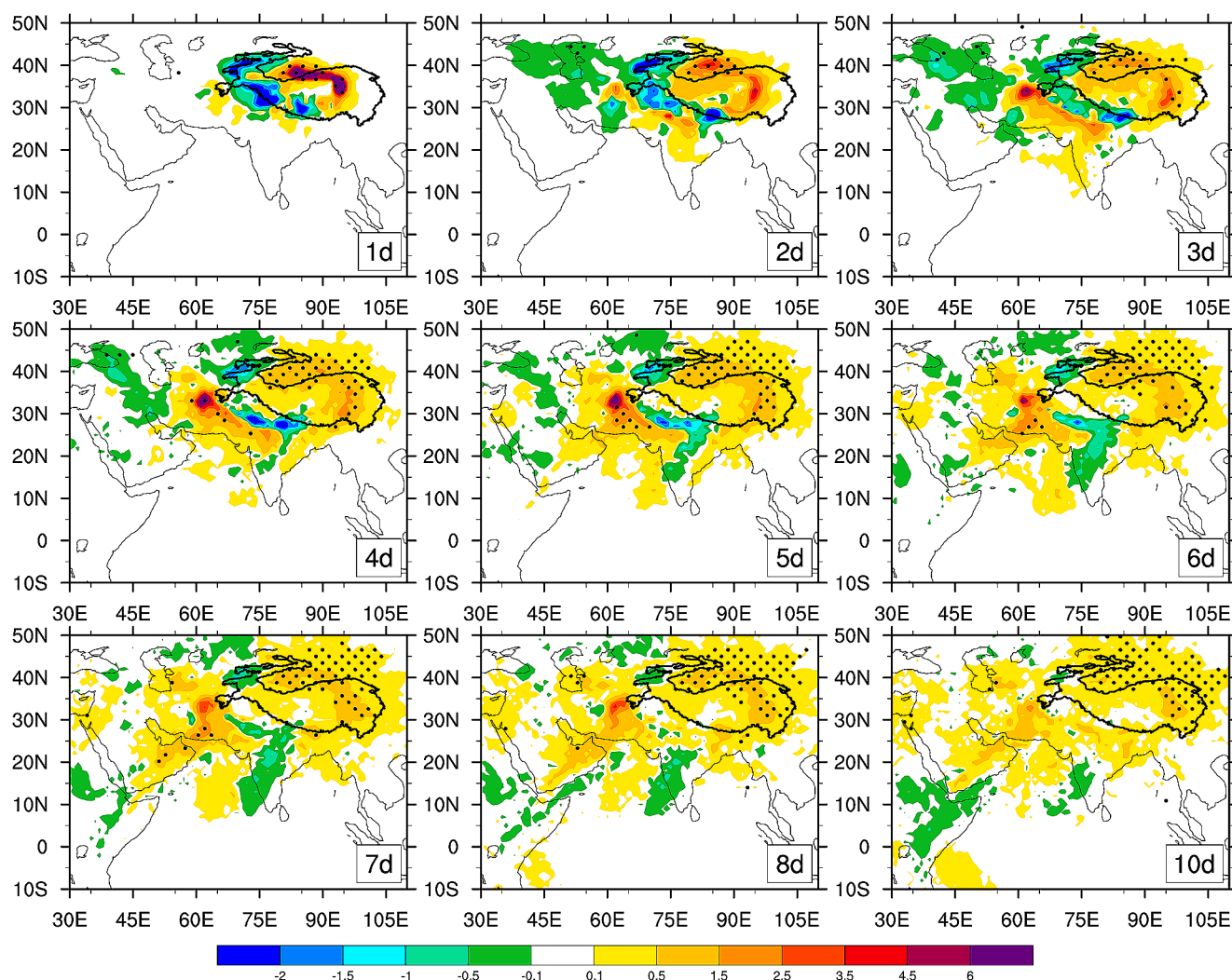


Fig. 14 Distributions of difference in moisture sources between P1 and P2 periods with respect to the different transport time scales (color shaded, $P2-P1$, $10^2 \text{mm}\cdot\text{day}^{-1}$). The 1d, 2d, 3d and so on representing the moisture sources $(E-P)_n$ derived from the corresponding back-

ward trajectories of separate day before the air parcels reaching the TRH region (The dotted area means the difference is statistically significant at the 95% confidence level)

multiple transport time scales (from 1 to 10 days). The Tibetan Plateau (TP), the Central Eastern Asian region (CEA), and the Arabian Peninsula (ARP) are ranked as the three leading contributors of the enhanced moisture supply, with the accumulated moisture sources on all grids increased by 11.3 (0.41%), 8.61 (0.52%) and 8.63 (0.33%) mm per year, respectively. This result implies that the terrestrial source plays a leading role in regulating the decadal shift of TRHR summer precipitation, rather than that directly from the oceanic regions. In particular, the relatively shorter transport time distance and steady contribution (lasting for 10 days) from the TP highlight the vital role of the enhanced local precipitation recycling process.

3) The Silk Road Index (SRI) and Indo-Pacific Warm Pool Index (WPI) tend to dominate the dipole pattern of

summer precipitation in the TRH region by influencing the west-east phase shift of the TP moisture contribution. The decadal variations in mid-latitude meridional winds and the low-latitude sea surface temperature SST bridge the changes in moisture sources and precipitation during the summer season. However, as mentioned above, the atmospheric circulation systems regulating the summer precipitation in TRH are rather intricate, and the changes in moisture changes over this region involve multiple factors. For instance, Sun et al. (2020) emphasized the weakening of the westerlies, which is connected to the Atlantic Multidecadal Oscillation, could make a significant contribution to the wetting of the Inner TP. The complexity of the variation in precipitation over the TRH region warrants further in-depth studies.

Acknowledgements We thank the Dr. Juan Huo and Chunzhu Wang for their valuable comments and English editing. This research was supported by National Key R&D Program of China (2023YFC3010700), the Second Tibetan Plateau Comprehensive Scientific Expedition and Research Program (2019QZKK0105), the S&T Development Fund of CAMS (2021KJ021; 2023KJ027), the State Key Laboratory of Severe Weather, Chinese Academy of Meteorological Sciences (2023LASW-A04), and Special Project for Innovation and Development of CMA (Grant: CXFZ2023J050).

Author contributions Bin Chen and Hongli Ren contributed to the study conception and design. Material preparation, data collection and analysis were performed by Ruiyu Zhao, Bin Chen and Yang Zhao. The draft of the manuscript was written by Bin Chen and Wei Zhang. All authors commented on first draft of the manuscript. All authors read and approved the final manuscript.

Data availability We acknowledge the National Meteorological Information Center (NMIC) of the China Meteorological Administration (NMIC/CMA) for producing the quality-controlled monthly precipitation data set, which can be obtained from <http://data.cma.cn/>. We also thank ECMWF for the ERA-interim data. The ERA-Interim dataset can be obtained from <http://www.ecmwf.int>. The Indo-Pacific Warm Pool Index is derived from NOAA (<https://psl.noaa.gov/data/climateindices/list/>). The model FLEXPART's source code and a manual are freely available from <https://www.flexpart.eu/>. The Lagrangian simulations subject of the present analysis can be obtained from the authors upon request.

Declarations

Ethical approval The authors certify that the study was performed in accordance with the Committee on Publication Ethics guidelines.

Competing interests The authors have no relevant financial or non-financial interests to disclose.

References

- Chen B, Xu XD, Yang S et al (2012) On the origin and destination of atmospheric moisture and air mass over the Tibetan Plateau. *Theor Appl Climatol* 110:423–435. <https://doi.org/10.1007/s00704-012-0641-y>
- Chen DL, Xu BQ, Yao TD et al (2015) Assessment of past, present and future environmental changes on the Tibetan Plateau. *Chin Sci Bull* 60(32):3023–3035
- Chen B, Zhang W, Yang S et al (2019) Identifying and contrasting the sources of the water vapor reaching the subregions of the Tibetan Plateau during the wet season. *Clim Dyn* 53:6891–6907
- Chen Y, Wen J, Liu R, Zhou J, Liu W (2022) The Characteristics of Water Vapor Transport and its linkage with summer precipitation over the source region of the Three Rivers. *J Hydrometeorol* 23:441–455. <https://doi.org/10.1175/JHM-D-21-0095.1>
- Curio J, Scherer D (2016) Seasonality and spatial variability of dynamic precipitation controls on the Tibetan Plateau. *Earth Syst Dyn* 7:767–782. <https://doi.org/10.5194/esd-7-7672016>
- Curio J, Maussion F, Scherer D (2015) A 12-year high-resolution climatology of atmospheric water transport over the Tibetan Plateau. *Earth Syst Dynam* 6:10925
- Dee DP et al (2011) The ERA-Interim reanalysis: configuration and performance of the data assimilation system. *Q J Roy Meteorol Soc* 137:553–597
- Dong YY, Zhai JQ, Zhao Y et al (2020) Teleconnection patterns of precipitation in the three-river Headwaters region, China. *Environ Res Lett* 15., Article 104050. <https://doi.org/10.1088/1748-9326/aba8c0>
- Feng L, Zhou T (2012) Water vapor transport for summer precipitation over the Tibetan Plateau: Multidata set analysis. *J Geophys Res: Atmos* 117:D20114
- Gao Y, Cuo L, Zhang Y (2014) Changes in moisture flux over the Tibetan Plateau during 1979–2011 and possible mechanisms. *J Clim* 27:1876–1893
- Gimeno L, Stohl A, Trigo RM et al (2012) Oceanic and terrestrial sources of continental precipitation. *Rev Geophys* 50:RG4003. <https://doi.org/10.1029/2012RG000389>
- Gimeno L, Vazquez M, Eirasbarca J et al (2020) Recent progress on the sources of continental precipitation as revealed by moisture transport analysis. *Earth Sci Rev* 201:103070
- Gimeno-Sotelo L, Gimeno L (2022) Where does the link between atmospheric moisture transport and extreme precipitation matter?. *Weather Clim Extrem*. <https://doi.org/10.1016/j.wace.2022.100536>
- Guo X, Feng Q, Si J, Zhang X (2022) Considerable influences of recycled moistures and summer monsoons to local precipitation on the northeastern tibetan Plateau. *J Hydrol* 605:127343
- He Y, Tian W, Huang J, Wang G, Ren Y, Yan H et al (2021) : The mechanism of increasing summer water vapor over the Tibetan Plateau. *Journal of Geophysical Research: Atmospheres*, 126, e2020JD034166. <https://doi.org/10.1029/2020JD034166>
- Held IM, Soden BJ (2006) Robust responses of the Hydrological cycle to global warming. *J Clim* 19:5686–5699. <https://doi.org/10.1175/JCLI3990.1>
- Huang NE, Shen Z, Long SR, Wu MC, Shih EH, Zheng Q, Tung CC, Liu HH (1998) : The empirical mode decomposition and the Hilbert spectrum for nonlinear and nonstationary time series analysis. *Proc. Roy. Soc. London*, 454A, 903–995
- Immerzeel WW, van Beek LPH, Bierkens MFP (2010) Climate change will affect the Asian water towers. *Science* 328:1382–1385. <https://doi.org/10.1126/science.1183188>
- Immerzeel WW, Lutz AF, Andrade M et al (2020) Importance and vulnerability of the world's water towers. *Nature* 577:364–369
- Jiang J, Zhou T, Qian Y et al (2023) Precipitation regime changes in High Mountain Asia driven by cleaner air. *Nature*. <https://doi.org/10.1038/s41586-023-06619-y>
- Kosaka Y, Nakamura H, Watanabe M, Kimoto M (2009) Analysis on the dynamics of a wave-like teleconnection pattern along the summertime Asian jet based on a reanalysis dataset and climate model simulations. *J Meteorol Soc Jpn* 87(3):561–580. <https://doi.org/10.2151/jmsj.87.561>
- Kukulies J, Lai HW, Curio J et al (2023) Mesoscale convective systems in the third Pole region: characteristics, mechanisms and impact on precipitation front. *Earth Sci* 11. <https://doi.org/10.3389/feart.2023.1143380>
- Lai HW, Chen HW, Kukulies J et al (2021) Regionalization of seasonal precipitation over the Tibetan Plateau and associated large-scale atmospheric systems. *J Clim* 34(7):2635–2651. <https://doi.org/10.1175/JCLI-D-20-0521.1>
- Lei YB, Yao TD, Bird BW et al (2013) Coherent lake growth on the central tibetan Plateau since the 1970s: characterization and attribution. *J Hydrol* 483:61–67. <https://doi.org/10.1016/j.jhydrol.2013.01.003>
- Lei YB, Yang K, Wang B, Sheng YW, Bird BW, Zhang GQ, Tian L (2014) Response of inland lake dynamics over the Tibetan Plateau to climate change. *Clim Change* 125:281290. <https://doi.org/10.1007/s10584-014-1175-3>
- Li S, Li D, Zhao P, Zhang G (2009) The climatic characteristics of vapor transportation in rainy season of the origin area of three

- rivers in Qinghai-Xizang Plateau. *Acta Meteor Sin* 67:591–598. <https://doi.org/10.11676/qxxb2009.059>
- Li S, Yao Z, Wang R et al (2020) Dryness/wetness pattern over the Three-River Headwater region: variation characteristic, causes, and drought risks. *Int J Climatol* 40:3550–3566. <https://doi.org/10.1002/joc.6413>
- Li X, Wu P, Ding Y, Liu Y, Li Q (2022) Spatial-temporal variation of precipitation recycling over the Tibetan Plateau under climate warming. *Atmos Res* 280:106431. <https://doi.org/10.1016/j.atmosres.2022.106431>
- Li J, Lu C, Chen J et al (2024) The influence of complex terrain on cloud and precipitation on the foot and slope of the southeastern Tibetan Plateau. *Clim Dyn*. <https://doi.org/10.1007/s00382-023-07056-3>
- Liu H, Duan K, Li M, Shi P, Yang J, Zhang X, Sun J (2015) Impact of the North Atlantic Oscillation on the Dipole Oscillation of summer precipitation over the central and eastern Tibetan Plateau. *Int J Climatol* 35(15):4539–4546
- Liu XZ, Wu Y, Liu et al (2019) Spatial-temporal characteristics of precipitation from 1960 to 2015 in the three Rivers' Headstream region, Qinghai, China. *Acta Geograph. Sin* 74:1803–1820. <https://doi.org/10.11821/dlxb201909008>
- Liu X, Liu, Yimin W, Xiaocong, and, Wu G (2020) : Large-Scale dynamics and Moisture sources of the Precipitation over the Western Tibetan Plateau in Boreal Winter. *J Geophys Research: Atmos.* (125), 9, 2169–8996
- Liu X, Yang MX, Dong NP Increased southerly and easterly water vapor transport contributed to the dry-to-wet transition of summer precipitation over the Three-River Headwaters in the Tibetan Plateau, *Advances in Climate Change Research*, 14(4):502–510., Liu R, Wang X, Wang ZL et al (2023) 2022: Atmospheric moisture sources of drought and wet events during 1979–2019 in the Three-River Source Region, Qinghai–Tibetan Plateau. *Theoretical and Applied Climatology*, 149:487–499. <https://doi.org/10.1007/s00704-022-04058-9>
- Ma YZ, Lu MQ, Chen HN et al (2018) Atmospheric moisture transport versus precipitation across the Tibetan Plateau: a mini-review and current challenges. *Atmos Res* 209:50–58
- Martin P, Hoerling J, Eischeid, Perlwitz J (2010) Regional Precipitation trends: distinguishing natural variability from anthropogenic forcing. *J Clim* 23:2131–2145
- Meng Xianhong M, Deng Y, Liu Z, Li L, Zhao (2022) : Remote Sensing-Detected Changes in Precipitation over the Source Region of Three Rivers in the Recent Two Decades, *Remote Sensing*, <https://doi.org/10.3390/rs14092216>, 14, 9, (2216)
- North GRTL, Bell RF, Cahalan et al (1982) Sampling errors in the estimation of empirical orthogonal functions. *Mon Weather Rev* 110(7):699–706
- Pan C, Zhu B, Gao J, Kang H, Zhu T (2019) Quantitative identification of moisture sources over the Tibetan Plateau and the relationship between thermal forcing and moisture transport. *Clim Dyn* 52:181–196
- Qian C, Zhou T (2014) Multiinterdecadal variability of North China aridity and its relationship to PDO during 1900–2010. *J Clim* 27(3):1210–1222
- Qiao BJ, Zhu LP, Yang RM (2019) Temporal-spatial differences in lake water storage changes and their links to climate change throughout the Tibetan Plateau. *Remote Sens Environ* 222:232–243. <https://doi.org/10.1016/j.rse.2018.12.037>
- Qiu J (2008) China: the third Pole. *Nature* 454:393–396. <https://doi.org/10.1038/454393A>
- Quan C, Chen B, Zhao T, Zhou B, Han Y (2016) Application of Lagrange water vapor source diagnosis method to the Three River Source Area. *J Appl Meteor* 27:688–697. <https://doi.org/10.11898/1001-7313.20160605>
- Rai D, Raveh-Rubin S (2023) Enhancement of Indian summer monsoon rainfall by cross-equatorial dry intrusions. *npj Clim Atmos Sci* 6:43. <https://doi.org/10.1038/s41612-023-00374-7>
- Shang W, Duan K, Ren X, Guo Y, Guan W, Li S ,2022: changes in the dominant mode of summer precipitation over the central-eastern Tibetan Plateau around the mid-1990s. *J Geophys Research: Atmos*, 127, e2022JD036617.
- Shao QQ, Cao W, Fan JW et al (2017) Effects of an ecological conservation and restoration project in the three-river source region, China. *J Geogr Sci* 27:183–204. <https://doi.org/10.1007/s11442-017-1371-y>
- Shi H, Li T, Wei J (2017) Evaluation of the gridded CRU TS precipitation dataset with the point raingauge records over the three-river headwaters. *Region J Hydrol* 548:322–332
- Sodemann H, Schwierz C, and H. Wernli (2008) Interannual variability of Greenland winter precipitation sources: lagrangian moisture diagnostic and north Atlantic Oscillation influence. *J Geophys Res* 113:D03107. <https://doi.org/10.1029/2007JD008503>
- Stohl A, and P. James (2004) A lagrangian analysis of the atmospheric branch of the global water cycle. Part I: method description, validation, and demonstration for the August 2002 flooding in Central Europe. *J Hydrometeorol* 5(8):656–678
- Stohl A, and P. James (2005) A lagrangian analysis of the atmospheric branch of the global water cycle. Part II: moisture transports between Earth's ocean basins and river catchments. *J Hydrometeorol* 6(12):961–984
- Stohl A, Seibert P (1998) : Accuracy of trajectories as determined from the conservation of meteorological tracers. *Q J R Meteorol Soc*, 124
- Sun B, Wang. HJ (2018) Interannual variation of the spring and summer precipitation over the Three River Source Region in China and the associated regimes. *J Clim* 18:7441–7457. <https://doi.org/10.1175/JCLI-D-17-0680.1>
- Sun J, Yang K, Guo W, Wang Y, He J, Lu H (2020) Why has the Inner Tibetan Plateau become wetter since the Mid-1990s? *J Clim* 33:8507–8522
- Sun Y, Yang C, Zhou S et al (2024) Possible mechanism of south-north reverse of early summer precipitation on the Tibetan Plateau. *Clim Dyn*. <https://doi.org/10.1007/s00382-024-07246-7>
- Tong LG, Xu XL, Fu Y et al (2014) Wetland changes and their responses to climate change in the three-river Headwaters region of China since the 1990s. *Energies* 7:2515–2534. <https://doi.org/10.3390/en7042515>
- Trenberth KE (1999) Atmospheric moisture recycling: role of advection and local evaporation[J]. *J Clim* 12:1368–1381. [https://doi.org/10.1175/1520-0442\(1999\)0122.0.CO;2](https://doi.org/10.1175/1520-0442(1999)0122.0.CO;2)
- Wang JY (2007) Analysis of the characteristics of water resources in the Sanjiangyuan of Qinghai Province. *J Water Resour Water Eng* NO. 71(01):91–94 (in chinese)
- Wang X, Pang G, Yang M (2018) Precipitation over the Tibetan Plateau during recent decades: a review based on observations and simulations. *Int J Climatol* 38:1116–1131. <https://doi.org/10.1002/joc.5246>
- Wang Z, Yang S, Luo H, Li J (2022) Drying tendency over the southern slope of the Tibetan Plateau in recent decades: role of a CGT-like atmospheric change. *Clim Dynam* 59:2801–2813
- Wang S, Huang J, Huang G, Luo F, Ren Y, He Y (2022b) Enhanced impacts of Indian Ocean sea surface temperature on the dry/wet variations over Northwest China. *J Geophys Research: Atmos*, 127, e2022JD036533.
- Wang ZL, Sun MP, Zhang MJ et al (2023) Enhanced atmospheric water cycle processes induced by climate warming over the three rivers source region. *Atmos Res* 295:107040
- Wu Z, Huang NE (2009) Ensemble empirical Mode Decomposition: a noise-assisted data analysis method. *Adv Adapt Data Anal* 1:1–41

- Xi Y, Miao C, Wu J, Duan Q, Lei X, Li H (2018) Spatiotemporal changes in extreme temperature and precipitation events in the three-Rivers Headwater region. *China J Geophys Res Atmos* 123:5827–5844
- Xu XD, Zhao TL, Lu CG et al (2014) An important mechanism sustaining the atmospheric water tower over the Tibetan Plateau. *Atmospheric Chem Phys* 14(20) 11, 287–11,295. <https://doi.org/10.5194/acp-14-11287-2014>
- Xu XD, Dong LL, Zhao Y et al (2019) Effect of the Asian water tower over the Qinghai–Tibet Plateau and the characteristics of atmospheric water circulation. *Chin Sci Bull* 64:2830–2841. <https://doi.org/10.1360/TB-2019-0203> (in Chinese)
- Xu X, Heng Z, Li Y, Wang S, Li J, Wang Y, Chen J, Zhang P, Lu C (2024) Improvement of cloud microphysical parameterization and its advantages in simulating precipitation along the Sichuan–Xizang Railway. *Sci China Earth Sci* 67:856–873. <https://doi.org/10.1007/s11430-023-1247-2>
- Xu X, Lu C, Shi X, Gao S (2008) World water tower: an atmospheric perspective. *Geophys Res Lett* 35(20):L20815
- Yang K, Wu H, Qin J, Lin C, Tang W, Chen Y (2014) Recent climate changes over the Tibetan Plateau and their impacts on Energy and Water cycle: a review. *Glob Planet Change* 112:79–91. <https://doi.org/10.1016/j.gloplacha.2013.12.001>
- Yang K, Lu H, Yue SY, Zhang GQ, Lei YB, La Z, Wang W (2018) Quantifying recent precipitation change and predicting lake expansion in the inner tibetan Plateau. *Clim Change* 147:149–163. <https://doi.org/10.1007/s10584-017-2127-5>
- Yang S, Zhang W, Chen B et al (2020) Remote moisture sources for 6-hour summer precipitation over the Southeastern Tibetan Plateau and its effects on precipitation intensity. *Atmos Res* 236. <https://doi.org/10.1016/j.atmosres.2019.104803>
- Yao T, and Coauthors (2019) Recent third Pole’s Rapid warming accompanies Cryospheric Melt and Water cycle intensification and interactions between Monsoon and Environment: Multidisciplinary Approach with observations, modeling, and analysis. *Bull Am Meteorol Soc* 100(3):423–444
- Yao TD, Coauthors (2012) Different glacier status with atmospheric circulations in Tibetan Plateau and surroundings. *Nat Clim Change* 2:663–667. <https://doi.org/10.1038/nclimate1580>
- Yao T, Bolch T, Chen D et al (2022) The imbalance of the Asian water tower. *Nat Rev Earth Environ* 3:618–632. <https://doi.org/10.1038/s43017-022-00299-4>
- Yi XS, Li GS, Yin YY (2013) Spatio-temporal variation of precipitation in the Three-River Headwater region from 1961 to 2010. *J Geogr Sci* 23:447–464. <https://doi.org/10.1007/s11442-013-1021-y>
- Yu RC, Li J, Zhang MM et al (2023) : South drying and north wetting over the Tibetan Plateau modulated by a zonal temperature dipole across timescales. *Adv. Clim. Change Res.*, 14 (2) (2023), pp. 276–285, <https://doi.org/10.1016/j.accre.2023.03.005>
- Yue S, Wang B, Yang K et al (2021) Mechanisms of the interdecadal variability of monsoon rainfall in the southern Tibetan Plateau. *Environ Res Lett* 16(1):014011. <https://doi.org/10.1088/1748-9326/abcb36>
- Zhang C, Tang Q, Chen D (2017) Recent changes in the moisture source of precipitation over the Tibetan Plateau. *J Clim* 30(5):1807–1819
- Zhang Y, Li T, Li J, Zhong D (2019a) Influence of the westerlies and the South Asia monsoon on water vapor transport and precipitation in the three-river Headwaters Region during the rainy season. *Adv Water Sci* 30:348–358
- Zhang Y, Huang W, Zhong D (2019b) Major Moisture Pathways and their importance to Rainy season precipitation over the Sanjiangyuan Region of the Tibetan Plateau. *J Clim* 32(20):6837–6857. <https://doi.org/10.1175/jcli-d-19-0196.1s>
- Zhang C, Tang Q, Chen D, van der Ent RJ, Liu X, Li W, Haile GG (2019c) moisture source changes contributed to different precipitation changes over the Northern and Southern Tibetan Plateau. *J Hydrometeorol*, 20(2), 217–229
- Zhao RY, Chen B, Xu XD (2021) Intensified moisture sources of heavy precipitation events contributed to Interannual Trend in Precipitation over the three-Rivers-Headwater Region in China. <https://doi.org/10.3389/feart.2021.674037>
- Zhao R, Chen B, Zhang W, Yang S, Xu X (2023) Moisture source anomalies connected to flood-drought changes over the three-rivers headwater region of Tibetan Plateau. *Int J Climatol* 43(12):5303–5316. <https://doi.org/10.1002/joc.8147>
- Zhou CY, Zhao P, Chen JM (2019) The interdecadal change of summer water vapor over the Tibetan Plateau and associated mechanisms. *J Clim* 32:4103–4119. <https://doi.org/10.1175/JCLI-D-18-0364.1>

Publisher’s Note Springer Nature remains neutral with regard to jurisdictional claims in published maps and institutional affiliations.

Springer Nature or its licensor (e.g. a society or other partner) holds exclusive rights to this article under a publishing agreement with the author(s) or other rightsholder(s); author self-archiving of the accepted manuscript version of this article is solely governed by the terms of such publishing agreement and applicable law.